International Society for Biofabrication
PURPOSE-LED PUBLISHING™

PAPER • **OPEN ACCESS**

A new microphysiological platform to study the permeation of neuroactive agents across intestinal and brain barriers

To cite this article: Barbara Pavan *et al* 2026 *Biofabrication* **18** 025013

View the article online for updates and enhancements.

You may also like

- Micro-comb 3D printing: rapid fabrication of tissue-guiding substrates using micro-embossed nozzles
Sarkhan Butdayev, Stefan Leone, Shayla Nikzad et al.
- Radial constraint of plastically compressed human dermo-epidermal skin substitutes mitigates *in vitro* contraction and enhances structural maturity
Luca Pontiggia, Jessica Polak, Vanuchija Someswaran et al.
- Biomechanical 3D tumor models on a micro-milled high-throughput force sensor array
Bashar Emon, Ahmadreza Kashefi, Md Habibur Rahman et al.

This content was downloaded from IP address 192.167.211.241 on 11/05/2026 at 16:45

Biofabrication

Check for updates

OPEN ACCESS

RECEIVED
11 July 2025

REVISED
4 March 2026

ACCEPTED FOR PUBLICATION
12 March 2026

PUBLISHED
25 March 2026

Original content from this work may be used under the terms of the Creative Commons Attribution 4.0 licence.

Any further distribution of this work must maintain attribution to the author(s) and the title of the work, journal citation and DOI.

PAPER

A new microphysiological platform to study the permeation of neuroactive agents across intestinal and brain barriers

Barbara Pavan[1,4], **Giada Botti**[2], **Alessandro Dalpiaz**[2,*], **Raffaello Sbordoni**[3], **Abdullah Talari**[3] and **Valon Llabjani**[3]

[1] Department of Neurosciences and Rehabilitation—Section of Physiology, University of Ferrara, Ferrara, Italy
[2] Department of Chemical, Pharmaceutical and Agricultural Sciences, University of Ferrara, Ferrara, Italy
[3] Revivocell Limited, I-TAC Bio Sci-Tech, Daresbury, United Kingdom
[4] Current address: CTNSC@UniFe, Italian Institute of Technology (IIT), Ferrara 44121, Italy.
[*] Author to whom any correspondence should be addressed.

E-mail: dla@unife.it

Keywords: microphysiological systems, physiological barriers, eugenol, dopamine, oral and intravenous administrations

Supplementary material for this article is available online

Abstract

To replicate key physiological barriers *in vitro*, we utilized the CELLBLOKS® modular microphysiological system. Specifically, human cerebral microvascular endothelial hCMEC/D3 cells, human retinal pigment epithelial cells, and rat small intestinal IEC-6 cells were grown in CELLBLOKS® to mimic the blood-brain (BBB), blood-cerebrospinal fluid (BCSFB), and intestinal (IB) barriers, respectively. Eugenol is an essential oil component known to permeate the central nervous system (CNS) *in vivo* after intravenous (IVA) and oral (OA) administrations; it was therefore used to simulate IVA and OA into the CELLBLOKS® system, using also celiprolol as negative control compound, since it is known for its poor ability to permeate in the CNS from the bloodstream. In particular, the IVA (systemic) of the compounds was simulated by their direct addition to the bloodstream-like lower channel of CELLBLOKS® (basolateral side of both BCSFB and IB; apical side for BBB), whereas their OA was simulated by apical addition to IEC-6. Permeation measurements, via High-performance liquid chromatography, across physiological barriers cultured in CELLBLOKS® demonstrated that, following both simulated oral and systemic administration, eugenol crosses the mimicked BBB and the BCSFB indiscriminately; conversely, the permeation of celiprolol across these barriers results strongly limited in comparison to eugenol. To assess downstream neuroactivity, dopaminergic neuron-like PC12 cells were cultured on NANOSTACKS™ inserts and incorporated into the BBB and BCSFB blocks. After simulated IVA and OA, significant eugenol-induced dopamine release by PC12 cells was evidenced both in BBB- and BCSFB-delimited neuronal-like compartments. These results validate the CELLBLOKS® and NANOSTACKS™ platforms as robust tools characterized by low costs, high reproducibility and ease of manipulation for *in vitro* studies of brain targeting of new drugs. This system requires two weeks culture period to be ready for the simulation *in vitro* of IB, BBB, BCFSB and neuronal tissues, appearing useful in limiting pre-clinical animal testing.

1. Introduction

Many biological barriers severely select the endogenous and exogenous molecules that can cross them to ensure the supply of essential nutrients to the organs and tissues of the body, allowing, at the same time, their protection from xenobiotics [1]. An important role of the intestinal mucosa barrier is to keep the invading pathogens (*i.e.* virus and bacteria) and toxins out the bloodstream. Analogously, specific protectors for the brain are the blood-brain barrier (BBB) and the blood-cerebrospinal fluid barrier (BCSFB), both able to prevent a great number of molecules from entering the central nervous system (CNS) from the bloodstream. These barriers are critical determinants of CNS homeostasis,

© 2026 The Author(s). Published by IOP Publishing Ltd

posing challenging barriers to the permeation of circulating solutes, including ions, biomolecules, drugs [2]. Multiple transporters endogenously expressed at the BBB and BCSFB act as influx or efflux carriers, that can, respectively, facilitate the delivery of several molecules in the CNS, or prevent drugs from achieving at central level therapeutic concentrations [2].

Eugenol, a main component of natural essential oils with potential neuroactive protective properties, was previously evidenced in our lab for its marked aptitude to permeate in the cerebrospinal fluid (CSF) of rats from their bloodstream [3]. This compound was therefore recruited for *in vitro* studies, where it evidenced its ability to increase cell viability and induce dopamine (DA) release according to a hormetic behaviour in neuronal differentiated PC12 cells [3]. Based on these properties, we propose here eugenol as a reference compound able to permeate in the CNS, in order to characterize a new system for *in vitro* studies of drug permeation across the BBB or the BCSFB after simulated intravenous (IVA) or oral (OA) administrations. In this work we describe an experimental design using the customizable commercial system CELLBLOKS® and NANOSTACKS™, which together are a new versatile microphysiological system (MPS) developed by Revivocell [4, 5], suitable for testing and identifying mixed combinations of cells that replicate physiological barriers defining specific microenvironments [6]. For the first time, CELLBLOKS® modular platform was used as an *in vitro* system to investigate complex physiological processes governing diffusion, permeation, and uptake of a potentially therapeutic compound across a set of compartments delimited by the intestinal barrier (IB) and by the BBB or BCSFB. The aim of this study is to identify whether eugenol permeates the CNS by discriminating between the BBB and BCSFB, after crossing the IB. Therefore, the CELLBLOKS® system is configured to simulate *in vitro* the ability of eugenol to cross the BBB or BCSFB from the bloodstream to central compartments after both an IVA and an OA, this last requiring firstly the crossing of the IB. To validate the applicability of the CELLBLOKS® system for this type of investigation, celiprolol is used as negative control compound, being a substrate of the efflux transporter P-glycoprotein (P-gp) and known to have poor ability to cross the biological barriers, in particular those between the bloodstream and CNS [7]. Finally, to evaluate whether eugenol can be neuroactive after crossing cerebral barriers, rat pheochromocytoma PC12 cells were differentiated to form a dopaminergic neuronal network on special NANOSTACKS™ inserts and placed into the CELLBLOKS® basolateral compartment of the BBB and in the apical compartment of the BCSFB (inside the blocks), both mimicking specific compartments of the CNS. Accordingly, the DA secretion by PC12 cells was compared when induced by eugenol permeated across BBB or BCSFB to propose the reliability of this *in vitro* predictive system in the challenging transition from the laboratory bench to clinical studies on neurodegenerative diseases.

2. Materials and methods

2.1. Materials

Human cerebral microvascular endothelial hCMEC/D3 cells (CLU512-A) were purchased from Tebu-bio Srl (Milan, Italy). The human retinal pigment epithelial (HRPE) cell line was generously provided by Professor Puttur Prasad from the Department of Biochemistry & Molecular Biology, Medical College of Georgia, Augusta, GA, USA. Rat normal small intestine IEC-6 cells (RRID:CVCL_0343) were obtained from Sigma-Aldrich (Milan, Italy). The PC12 cell line (RRID:CVCL_0481), derived from rat adrenal gland pheochromocytoma, was kindly provided by Dr Federica Brugnoli from the University of Ferrara, Department of Translational Medicine, Italy. Dulbecco's Modified Eagle's Medium (DMEM), MCDB131 medium, Dulbecco's Modified Eagle's and Ham's F12 media (DMEM/F12), RPMI-1640 medium, nerve growth factor (NGF), fetal bovine serum (FBS), horse serum (HS), penicillin/streptomycin, and all the others cell culture reagents were from ThermoFisher Life Technologies (Milan, Italy) and Microtech (Naples, Italy). Paraformaldehyde phosphate-buffered saline (PFA; J61899.AK; Thermo Scientific, Milan, Italy), rabbit monoclonal ZO-1 antibody (GeneTex Cat# GTX636491, RRID:AB_2909994), rabbit polyclonal occludin antibody (GeneTex Cat# GTX114949, RRID:AB_11177242), Fluorescein (FITC) AffiniPure polyclonal Goat Anti-Rabbit IgG (Jackson ImmunoResearch Labs Cat# 111-095-003, RRID:AB_2337972), goat anti-Rabbit IgG H&L polyclonal antibody Rhodamine Conjugated (TRITC) (Abcam Cat# ab6718, RRID:AB_955551), and glycerol antifade mounting medium (Abcam Cat# ab188804) containing 4',6-Diamidino-2-phenylindole (DAPI) were purchased from Prodotti Gianni Srl (Milan, Italy).

CELLBLOKS® is a patented (GB2553074B), open-top multi-chambered organs-on-a-chip device designed by Revivocell (Daresbury, Warrington, UK). High-performance liquid chromatography (HPLC)-grade acetonitrile (CH_3CN) and methanol (MeOH) were acquired from Carlo Erba Reagents S.A.S. (Milan, Italy). Merck Life Sciences Srl (Milan, Italy) supplied eugenol (MW 164.21 g mol^{-1}), celiprolol hydrochloride (MW 415.95 g mol^{-1}), Dulbecco's Phosphate Buffered Saline (DPBS), phosphoric acid, dimethyl sulfoxide (DMSO), triton X-100, bovine serum albumin (BSA, A4503), and all other reagents

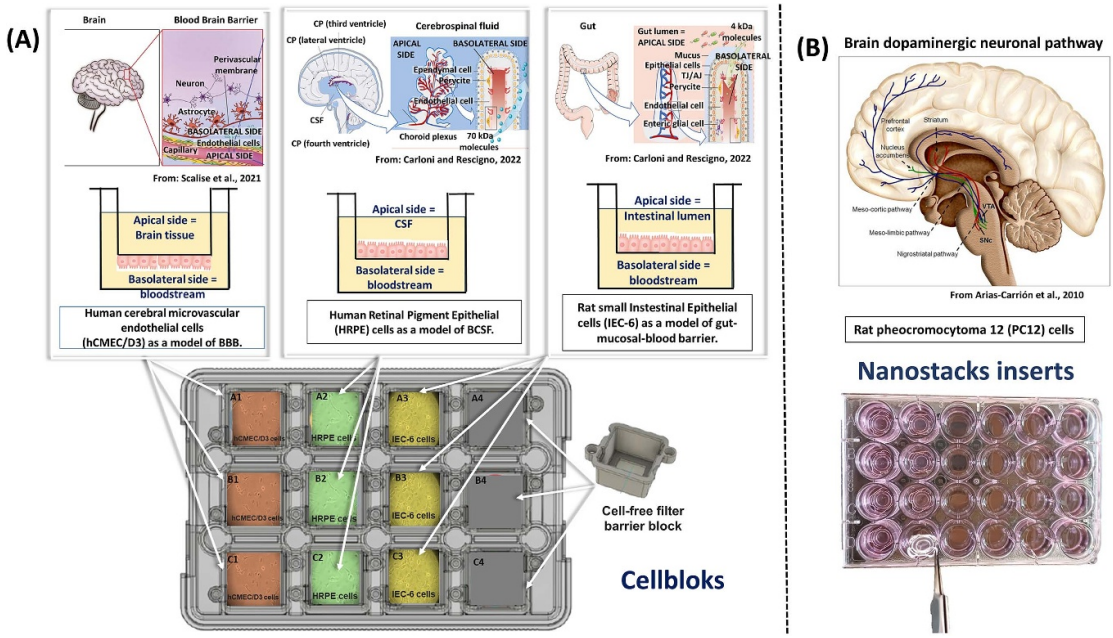

Figure 1. Schematic organisation of the CELLBLOKS® system for the growth and polarisation of hCMEC/D3 endothelial cells, IEC-6 epithelial cells, and HRPE epithelial cells to obtain confluent cell monolayers (A). Each cell type was grown using a unique channel, that was isolated from the others to be fed by its specific medium both in apical and in basolateral compartment. (B) Neuronal-like PC12 cells were grown separately in NANOSTACKS™ inserts, placed in a 24-well plate. Reproduced from [8]. CC BY 2.0. Reproduced from [9], with permission from Springer Nature. Reproduced with permission from [10]. © 2021 The Author(s), taken from Tissue Barriers © 2021 Taylor & Francis Group, reprinted by permission of Informa UK Limited, trading as Taylor & Francis Ltd, www.tandfonline.com. This is an open access article distributed under the terms of the creative commons attribution-noncommercial-noderivatives license (http://creativecommons.org/licenses/by-nc-nd/4.0/), which permits non-commercial re-use, distribution, and reproduction in any medium, provided the original work is properly cited, and is not altered, transformed, or built upon in any way.

or solvents not mentioned here. Purified water (H_2O) suitable for HPLC analysis was obtained using Sartorius Arium Advance EDI system (Sartorius Lab Instruments GmbH and Co., KG, Göttingen, Germany).

2.2. Use of CELLBLOKS® system for growing BBB, BCSFB and IB in vitro models

The CELLBLOKS® system was used differently for two distinct phases of the experimental design.

The first phase (figure 1) involved the seeding of cells and their growth as polarized cell monolayers (figure 1(A)) mimicking the BBB (obtained by hCMEC/D3 endothelial cells), BCSFB (obtained by HRPE epithelial cells), and IB (obtained by IEC-6 epithelial cells) on barrier blocks (1.0 μm pore size polyethylene terephthalate—PET—filter membranes) of CELLBLOKS® system. Moreover, this phase also included parallel seeding, growth, and dopaminergic neuronal-like differentiation of PC12 cells on NANOSTACKS™ (1.0 μm pore size PET filter membranes) inserted in a 24-well plate (figure 1(B)). This first phase was performed under static conditions. The epithelial/endothelial cell growth media were changed every other day, whereas the differentiation medium of PC12 cells was changed every 4 d.

The second phase (figure 2) focused on the use of the polarized cell monolayers to simulate *in vitro* the uptake in the CNS of test compounds (eugenol or celiprolol) after their IVA or OA, studying their ability to permeate across IB, BBB or BCSFB (figures 2(A) and (B)). To perform this phase, the barrier blocks were transferred from the CELLBLOKS® system used for their growth and rearranged in a new CELLBLOKS® platform, as represented in figure 2. DPBS supplemented with 5.3 mM glucose, 0.5 mM $MgCl_2$, 0.9 mM $CaCl_2$ was used as incubation buffer for the permeation experiments.

Moreover, this phase was completed by the inclusion of NANOSTACKS™ (1.0 μm pore size PET filter membranes) containing dopaminergic neuronal-like differentiated PC12 cells in both the BBB and BCSFB compartments to verify the potential ability of eugenol to stimulate DA release from PC12 cells, once it reached BBB and BCSF compartments after simulated IVA and OA (figure 2(C)). DPBS supplemented with 5.3 mM glucose, 0.5 mM $MgCl_2$, 0.9 mM $CaCl_2$, 1.0 mM ascorbic acid, 10 μM pargyline as monoamine oxidase inhibitor, and 1.0 μM nomifensine, as DA transporter inhibitor was used as incubation buffer for the baseline and eugenol-induced DA release experiments.

For the first experimental phase, the density suitable for cell seeding in CELLBLOKS® was obtained using a Scepter 2.0 cell counter (Merk-Millipore, Milan, Italy). Each of the three cell types was grown

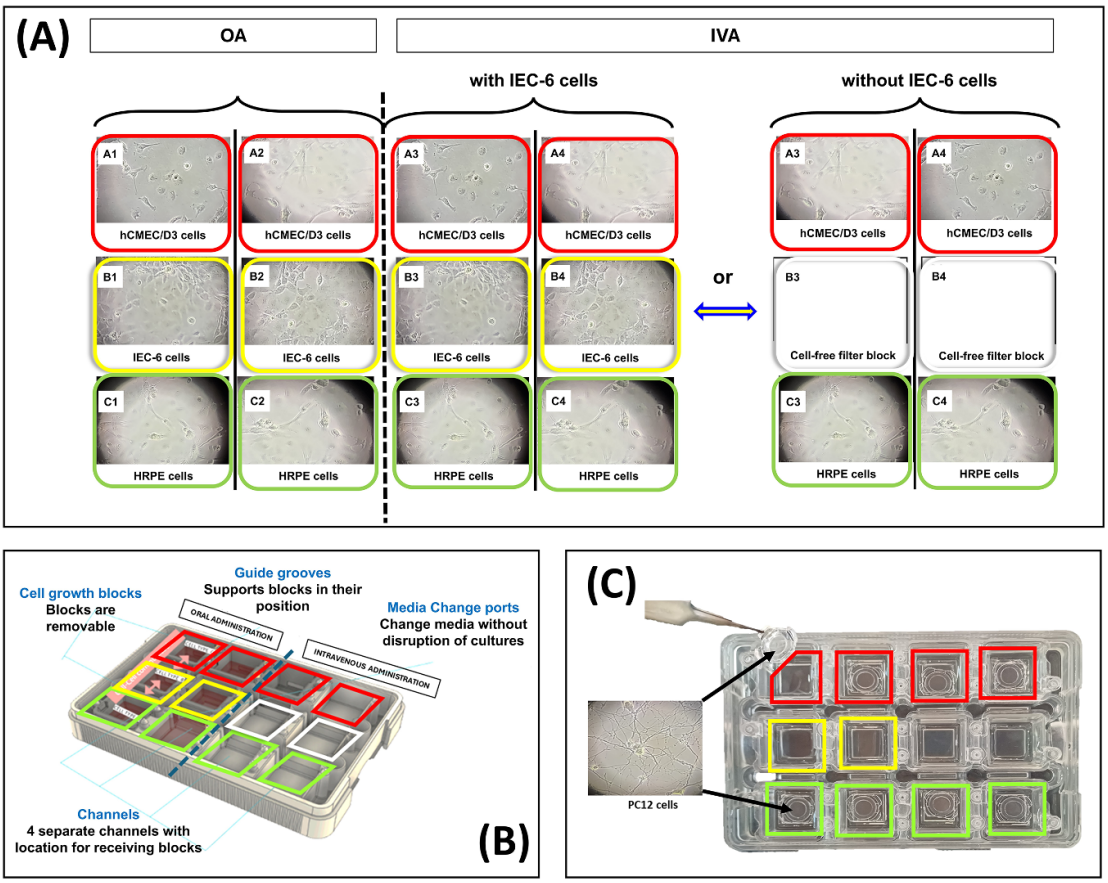

Figure 2. Arrangement of the CELLBLOKS® system. (A) Organisation of the channels of CELLBLOKS® system to simulate intravenous (IVA) or oral (OA) administrations and uptake in the CNS. Each channel mimicked the bloodstream. The barrier blocks, showing the hCMEC/D3, IEC-6, and HRPE cell monolayers, were inserted in the channel for simulated oral study; for the intravenous simulated study, the barrier block including IEC-6 cells was present (with IEC-6 cells) or substituted by a barrier block without cells (without IEC-6 cells). (B) CELLBLOKS® system showing in 3D the rearranged blocks for experimental set-up simulating IVA and OA. The double pink arrows indicate a single continuous channel underlying the blocks. (C) NANOSTACKS™ containing neuronal-like differentiated PC12 cells were transferred from the 24-well plate inside the BBB and BCSFB barrier blocks (corresponding to the neural compartments) of the CELLBLOKS® system used for the second phase of the experimental design. The two rows of CELLBLOKS® for each simulation type indicate experimental duplicates.

in a single channel of the CELLBLOKS® system (as represented in figure 1(A)) containing its specific apical and basolateral medium as the optimal growth condition (see below). Upon seeding, all the three types of cells developed tight and polarized confluent monolayers (as indicated by measurements of transepithelial/transendothelial electrical resistance—TEER and by immunofluorescence staining of junctional proteins, see below), which can be considered as physiologically active cell culture models of IB, BCSFB and BBB. The seeding and grown details for any type of cells are described in the following sections.

2.2.1. Human cerebral microvascular endothelial cell (hCMEC/D3) line

Endothelial hCMEC/D3 cells were routinely grown up to confluence in 100 μg ml^{-1} collagen I-coated T25 flasks containing MCDB131 medium supplemented with 5% FBS, 100 μg ml^{-1} streptomycin, 100 U ml^{-1} penicillin, 2 mM glutamine, 1 ng ml^{-1} bFGF, 5 μg ml^{-1} ascorbic acid, and 2 μM hydrocortisone, at 37 °C in 5% CO_2/95% humidified atmosphere. Reversed CELLBLOKS® barrier blocks, coated on their filter membrane with 200 μl of 100 μg ml^{-1} collagen I, were placed overnight in a 6-well plate at 37 °C and 95%-humidified atmosphere with 5% of CO_2. Then, each 100 μg ml^{-1} collagen I-coated CELLBLOKS® barrier block was rinsed with DPBS, and, after the first passage in culture, hCMEC/D3 cells were seeded by adding a drop of 300 μl containing 1 $\times$ 10^5 cells to the 100 μg ml^{-1} collagen I-coated membrane of reversed barrier blocks (1.0 μm pore size PET filter membranes), which were placed into a 6-well plate at 37 °C/5% CO_2 for 2 h for cell adhesion. The reversed block with adherent cells was then rightly repositioned into the dedicated channel of CELLBLOKS® system (for example channel 1 represented in figure 1(A)), with the apical/luminal domain of the cell membrane facing the channel (equivalent to the blood vessel lumen *in vivo*), containing 4 ml of MCDB131 complete medium, and the basolateral/abluminal

domain of the cell membrane facing the inside of the block (comparable to the CNS compartment *in vivo*) filled with 1 ml of MCDB131 complete medium (figure 1(A)). The hCMEC/D3 cells were then allowed to grow and differentiate as a tight monolayer of apicobasal-polarized brain endothelial cells.

2.2.2. HRPE cell line

HRPE cells were routinely grown at 37 °C in 5% CO_2/95% humidified atmosphere in tissue culture flasks up to confluence in 1:1 mixture of Dulbecco's Modified Eagle's and Ham's F12 medium (DMEM/F12), supplemented with 10% FBS, 2 mM glutamine, 100 μg ml^{-1} streptomycin and 100 U ml^{-1} penicillin. After the first passage in culture, HRPE cells were seeded directly inside the barrier blocks (1.0 μm pore size PET filter membranes), positioned in the dedicated channel of CELLBLOKS® system (for example channel 2 represented in figure 1(A)), at a density of 9×10^4 cells ml^{-1}, with the apical/luminal membrane domain facing the inside of the block (comparable to the CSF compartment *in vivo*), containing 1 ml of DMEM/F12 complete medium, and the basolateral/abluminal membrane domain facing the channel (comparable to the blood vessel lumen *in vivo*), containing 4 ml of DMEM/F12 complete medium (figure 1(A)). The cells were allowed to grow and differentiate to a tight monolayer of apicobasal polarized epithelial cells, expressing strong analogies with brain choroidal plexus epithelial barrier [11], being a pigmented monolayer of cells that comprises the entire blood outer blood-retinal barrier between the choroidal vascular plexus and the neurosensory retina [12].

2.2.3. Intestinal IEC-6 cell line

IEC-6 cells were routinely grown in DMEM medium containing Glutamax, 10% FBS, 100 μg ml^{-1} streptomycin, and 100 U ml^{-1} penicillin at 37 °C in a 95%-humidified atmosphere, with 5% of CO_2. After one passage, cells were seeded directly inside the barrier blocks (1.0 μm pore size PET filter membranes), positioned in the dedicated channel of CELLBLOKS® system (for example channel 3 represented in figure 1), at a density of 8×10^4 cells ml^{-1}, with the apical/luminal membrane domain facing the inside of the block (comparable to the intestinal lumen *in vivo*), containing 1 ml of DMEM complete medium, and the basolateral/abluminal membrane domain facing the bloodstream-like channel, containing 4 ml of DMEM complete medium (figure 1(A)), and allowed to reach the full IB function.

2.3. Evaluation of the integrity of cell monolayers

2.3.1. Transepithelial/transendothelial electrical resistance (TEER)

The reproducible barrier integrity obtained in the three cell lines was assessed by TEER measurement using a chopstick electrode linked to a voltmeter (Millicell-ERS, Merk-Millipore, Milan, Italy). TEER values for the cell monolayers were obtained by subtracting the intrinsic resistance (blank barrier block membrane) from the total resistance (barrier block membrane with cells) and adjusting for the surface area (Ω cm^2). HRPE cells and IEC-6 cell monolayers reached TEER stable values of 60 ± 2.5 Ω cm^2 and 69 ± 6.5 Ω cm^2, respectively, after 8 d of culture, while hCMEC/D3 cells reached similar TEER stable values (72 ± 9.5 Ω cm^2) after 12 d of culture; for this reason, hCMEC/D3 cells were seeded 3 d before HRPE and IEC-6 cells, so that all the monolayers reached stable values of TEER to be used for the transport studies at the same day.

2.3.2. Immunofluorescence staining

Barrier integrity was also validated by imaging the tight junctions connecting adjacent cells. IEC-6, hCMEC/D3, and HRPE cells were grown as confluent monolayer in CELLBLOKS® as described above and stained for the tight junction associated proteins zona occludens 1 (ZO-1) and occludin antibodies. Cell monolayers were washed three times with DPBS supplemented with 0.9 mM $CaCl_2$ and 0.5 mM $MgCl_2$, then fixed using 4% PFA for 15 min at room temperature (RT), followed by three wash steps with DPBS for 1 min. Subsequently, cell monolayers were permeabilized with 0.1% Triton X-100 (Merck, Milan, Italy) in DPBS for 5 min; then, cells were washed three times with PBS and incubated with a blocking solution containing 2% BSA in DPBS for 60 min at RT. IEC-6, hCMEC/D3, and HRPE cell monolayers were stained separately with each of the primary antibodies, i.e. rabbit monoclonal ZO-1 antibody diluted 1:500 in blocking buffer and rabbit polyclonal occludin diluted 1:200 in blocking buffer, all of them incubated for 2 h at RT.

Cell monolayers were then washed three times with PBS and incubated for 2 h at RT with secondary antibodies, i.e. FITC AffiniPure polyclonal Goat Anti-Rabbit IgG and TRITC Goat anti-Rabbit IgG H&L polyclonal antibody, both diluted 1:100 in blocking buffer.

A control without primary antibody was also performed to exclude autofluorescence or unspecific binding of the secondary antibody. All incubation and washing steps were performed on a rocker platform (8 angle) at RT. Then, each filter membrane was carefully cut along the basolateral edge of the insert with a sharp scalpel, using tweezers to remove

and prevent membrane from curling, and placed onto a microscope slide with the cells facing up. Cell monolayers were finally embedded in 100 μl of glycerol antifade mounting medium containing DAPI for nuclear counterstaining, covered with coverslips, and stored in the dark at 4 °C until image acquisition with a Nikon Eclipse Ts2-FL inverted microscope for multicolour imaging supported by NIS-Elements software (Balsamo Strumenti, Bologna, Italy). Image processing was performed using ImageJ 1.54p software (Image Processing and Analysis in Java; available at https://imagej.net/ij/download.html).

2.4. PC12 cells culture and differentiation to neuronal phenotype in CELLBLOKS® NANOSTACKS™ inserts

PC12 cells were grown in 4 μg cm^{-2} collagen IV-coated flasks containing RPMI-1640 medium containing Glutamax, supplemented with 100 μg ml^{-1} streptomycin, 100 IU ml^{-1} penicillin, 10% HS, and 5% FBS at 37 °C in 95% humidified atmosphere and 5% of CO_2. PC12 cells were gently detached with a rubber scraper, transferred as cell suspension into a Falcon tube and resuspended through a sterile tip to avoid any clumping, then split into separate flasks twice weekly. As shown in figure 1(B), NANOSTACKS™ (1.0 μm pore size PET filter membranes), coated in their inside filter membrane with 100 μl of 100 μg ml^{-1} collagen IV, were placed overnight in a 24-well plate at 37 °C and 95%-humidified atmosphere with 5% of CO_2. Then, each 100 μg ml^{-1} collagen IV-coated NANOSTACKS™ was rinsed with DPBS, and a 100 μl drop containing 2.5 $\times$ 10^3 PC12 cells was added to the inside of NANOSTACKS™ and left to adhere for 2 h at 37 °C in the incubator; then, 1 ml of complete RPMI-1640 medium was slowly added up to each NANOSTACKS™ containing PC12 cells. The next day, adherent cells were washed once with serum-free DMEM medium containing Glutamax and then switched to DMEM containing Glutamax medium supplemented with 100 ng ml^{-1} nerve growth factor (NGF) and 1% HS up to 14 d of differentiation period, visually displayed by the high occurrence of axonal extensions. At this time, NANOSTACKS™ were transferred from the 24-well plate inside the barrier blocks (corresponding to the neural compartments) of the CELLBLOKS® system used for the second phase of the experimental design (figure 2(C)). To obtain differentiated neuronal cells at the same time of the complete differentiation of the three monolayers mimicking the physiological barriers, PC12 cells were seeded on NANOSTACKS™ 5 d before hCMEC/D3 cells and 7 d before HRPE and IEC-6 cells.

2.5. Experimental design to simulate intravenous or OA of neuroactive compounds and their uptake in the CNS

In the second phase of the experimental design, all the barrier blocks containing tight cell polarized monolayers (obtained in the first experimental phase) were rearranged into a new CELLBLOKS® plate, to test in parallel the compounds (eugenol or celiprolol) after their simulated IVA and OA (figures 2(A) and (B)). Specifically, as shown in figure 2(A), each channel of the CELLBLOKS® systems contained up to three barrier blocks; the channels designed to replicate IVA or OA featured the barrier block with the IEC-6 epithelial monolayer positioned centrally, flanked by barrier blocks containing the hCMEC/D3 endothelial monolayer or the HRPE epithelial monolayer above and below; moreover, a further channel organisation to simulate the IVA was designed by replacing the barrier block containing the IEC-6 epithelial monolayer with a barrier block devoid of cells. For the investigations into the potential neuroactivity of eugenol following its permeation through the BBB or BCSFB, the NANOSTACKS™ containing neuronal-like differentiated PC12 cells were transferred from the 24-well plate into the BBB and BCSFB barrier blocks (corresponding to the neural compartments) of the CELLBLOKS® system used in the second phase of the experimental design (see figure 2(C)).

The CELLBLOKS® system built as described above allowed to design two sets of experiments (figure 3), that were performed in DPBS, supplemented with 5.3 mM glucose, 0.5 mM $MgCl_2$, 0.9 mM $CaCl_2$, by using celiprolol or eugenol. Stock solutions of these compounds were previously prepared by dissolving them in DMSO at the final concentration 10^{-2} M. The stock solutions were stored at −20 °C until their use, when they were diluted at the final concentrations of 7.5 μM or 25 μM in DPBS supplemented with 5.3 mM glucose, 0.5 mM $MgCl_2$ and 0.9 mM $CaCl_2$. Before the incubation with eugenol or celiprolol, CELLBLOKS® were washed thrice with pre-warmed DPBS buffer in the apical (1 ml) and basolateral (4 ml) sides of blocks. In the first set (figures 3(A) and (B)), IVAs of eugenol (used as test compound) or celiprolol (used as negative control compound) were simulated by individually spiking each compound (7.5 μM final concentration) directly in the lower bloodstream-like channel and measuring their amount in the BBB (hCMEC/D3 cells, simulating the permeation in the brain interstitial fluid) and BCSFB (HRPE cells, simulating the permeation in the CSF) CNS-like compartments after 60 min and 120 min. In particular, to simulate IVA, the CELLBLOKS® channels were arranged in two distinct configurations: one featuring intestinal IEC

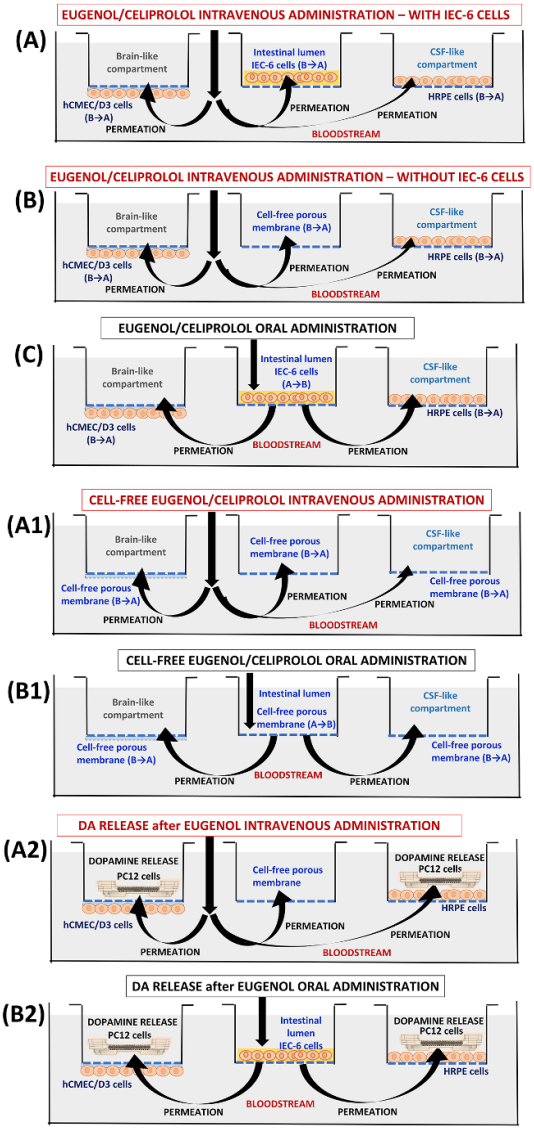

Figure 3. Scheme of experimental design. (A) *In vitro* simulation of intravenous administration (IVA) to study the permeation of eugenol or celiprolol across the simulated BBB and BCSFB in the presence of the IEC-6 intestinal monolayer. (B) *In vitro* simulation of IVA to study the permeation of eugenol or celiprolol across the simulated BBB and BCSFB in the absence of the IEC-6 intestinal monolayer. (C) *In vitro* simulation of oral administration (OA) to study the permeation of eugenol or celiprolol across intestinal IEC-6 cells and then, their permeation across BBB and BCSFB simulated by hCMEC/D3 and HRPE cell monolayers, respectively. Replication of simulated IVA (A1) and OA (B1) using cell-free barrier blocks to evaluate the background permeation across the porous membranes. (A2) *In vitro* simulation of IVA of eugenol targeting neuronal-like PC12 cells differentiated on permeable membrane of NANOSTACKS™ inserts after crossing the simulated BBB or BCFSB. (B2) Neuronal-like PC12 cells differentiated on permeable membrane of NANOSTACKS™ inserts and targeted by eugenol after its simulated OA and permeation firstly across intestinal IEC-6 cells, then across the simulated BBB or BCSFB.

monolayers (figure 3(A)) and the other consisting of a barrier block without cells (figure 3(B)), both positioned in the central rows (figure 2(A)). Additionally, the amounts of the compounds were assessed in the IEC-6 intestinal-like compartment after 60 and 120 min (figure 3(A)).

In parallel, tight monolayers of IEC-6 cells, grown inside the barrier blocks, allowed also to study the simulated oral permeation of eugenol or celiprolol (figure 3(C)). In this case, each compound (25 μM final concentration) was singularly spiked in the apical side of IB (IEC-6 cells, simulating the intestinal lumen) to permeate in the lower bloodstream-like channel and, after 60 min and 120 min, was tested for its ability to permeate across both BBB (hCMEC/D3 cells) and BCSFB (HRPE cells), being quantified via HPLC (see below) in their CNS-like compartments.

The TEER values of each monolayer were monitored before and after 120 min of incubation with the compounds. Both IVA and OA were replicated in another CELLBLOKS® plate using cell-free barrier blocks to calculate the background permeation across the porous membranes (figures 3(A1) and (B1)).

In the second experimental set (figures 3(A2) and (B2)), neuronal-like differentiated PC12 cells were used to simulate the dopaminergic branch of the CNS compartment, in which to evaluate whether the eugenol amounts able to cross BBB and/or the BCSFB may be suitable to elicit DA release. In this aim, neuronal-like differentiated PC12 cells in NANOSTACKS™ kept in a 24-well plate were entrained by applying a serum shock (50% HS and 50% DMEM containing Glutamax) for 2 h to synchronize the subsequent release of DA at the same time in all cells. PC12 cells in NANOSTACKS™ were then rinsed with DPBS and transferred inside the BBB and BCSFB blocks containing 1 ml of DPBS (supplemented with 5.3 mM glucose, 0.5 mM $MgCl_2$, 0.9 mM $CaCl_2$, 1.0 mM ascorbic acid, 10 μM pargyline as monoamine oxidase inhibitor, and 1.0 μM nomifensine, as DA transporter inhibitor) at 37 °C. Eugenol was spiked in the apical side of IEC-6 cells for simulated OA (figure 3(A1)) or in the basolateral chamber for simulated IVA (figure 3(A2)), as described for permeation experiments of the first set. For the quantification of baseline DA release, an equivalent CELLBLOKS® system was built as described for the second experimental set, avoiding the addition of eugenol.

After 60 and 120 min, 200 μl of DPBS were withdrawn from the inside of BBB and BCSFB blocks and centrifuged at 1000 × g for 20 min at 4 °C to remove cell debris, then stored at −20 °C using an enzyme-linked immunosorbent assay (ELISA) assay, as previously reported [3].

2.6. ELISA

The baseline DA levels and eugenol-stimulated DA levels were harvested in 200 μl DPBS samples after 60 min and 120 min of incubation to be analysed by means of the ELISA, based on the sandwich principle for DA detection, following the manufacturer's instructions (IBL International, Hamburg,

Germany–catalogue no: RE59161; purchased from Tecan Italia S.r.I, Milan, Italy). After the substrate reaction, the intensity of the developed colour was proportional to the DA amount, detected at 450 nm using a microplate reader spectrophotometer (NeoBiotech NB-12-0035 Microplate Reader, CliniSciences Srl, Guidonia Montecelio, Italy). Results were determined using a standard curve and expressed as mean ± SEM values of four independent experiments. Data were plotted and analysed with GraphPad Prism version 8.0 (GraphPad software, San Diego, CA, USA).

2.7. HPLC analysis

Eugenol and celiprolol concentrations in the apical and basolateral compartments of CELLBLOKS® systems were measured by HPLC, by using a modular system composed of an LC-40D pump and an SPD-M40 DAD detector (Shimadzu, Kyoto, Japan), and completed with an injection valve provided by a 20 μl sample loop (model 7725, Rheodyne, IDEX, Torrence, CA, USA). Data were acquired and processed using LabSolutions Software (version 5.110 in Windows 10, Shimadzu, Kyoto, Japan) installed on a personal computer.

For eugenol quantification, separations were performed at RT using a Hypersil BDS C18 column (5 μm, 150 mm × 4.6 mm i.d.) furnished by Thermo Fisher Scientific Italia (Milan, Italy) protected by a guard column packed with the same separation material. The mobile phase consisted of a mixture of water and acetonitrile 50:50 (v/v), with a flow rate set at 1 ml min^{-1}. The chromatograms resulting from the analysis were displayed at 210 nm, and the retention time of eugenol in these analytical conditions was 4.2 min.

For celiprolol quantification, separations were performed at RT using a Force Biphenyl column (150 × 4.6 mm, 5 μm) furnished by Restek (Milan, Italy) protected by a guard column packed with the same separation material. The mobile phase consisted of a mixture of phosphoric acid in water (0.2% v/v) and methanol 40:60 (v/v), with a flow rate set at 1 ml min^{-1}. The chromatograms resulting from the analysis were displayed at 232 nm, and the retention time of celiprolol in these analytical conditions was 3.6 min.

The chromatographic precisions for eugenol and celiprolol were evaluated by repeated analysis (10 μl, $n = 6$) of the same sample (10 μM) of eugenol (1.64 μg ml^{-1}) or celiprolol (3.79 μg ml^{-1}) singularly dissolved in DPBS, obtaining relative standard deviation values of 0.88% and 0.87%, respectively. The calibration curves of peak areas versus concentration of eugenol and celiprolol were obtained in a range from 0.1 μM to 50 μM (0.016–8.21 μg ml^{-1} for eugenol; 0.038–18.97 μg ml^{-1} for celiprolol) for both compounds singularly dissolved in DPBS and resulted linear in the considered range ($n = 9$, $r = 0.999$; $P < 0.0001$).

2.8. Statistical analysis

Statistical comparison among TEER values of the endothelial/epithelial cell monolayers before the experiments of transport of compounds was performed by one-way analysis of variance (ANOVA) followed by Tukey's multiple comparison test. Statistical comparison among eugenol and celiprolol concentrations detected after 60 min and 120 min both in simulated OA and IVA in the CELLBLOKS® inserts and statistical comparison among eugenol-induced DA release from PC12 cells in NANOSTACKS™ inserts after 60 min and 120 min both in simulated OA and IVA were performed by two-way ANOVA followed by Dunnett's and Tukey's multiple comparison tests. Values were expressed as mean ± SEM and $P < 0.05$ was considered statistically significant. Statistical analyses were performed using GraphPad Prism version 8.0 (GraphPad Software, San Diego, CA, USA).

3. Results

3.1. Assessment of IEC-6, hCMEC/D3 and HRPE cell monolayers integrity: TEER measurement and immunofluorescence staining of junctional proteins

Before transport studies, the tight junction integrity of cell monolayers growing on CELLBLOKS® system was tested by TEER measurements. In particular, the cell monolayers were considered suitable for permeation experiments when their TEER values reached a plateau, requiring 8 d for epithelial cells and 12 d for endothelial cells. As reported in figure 4, the three types of cell monolayers reached plateau TEER values that were not significantly different from each other, ranging between 60 and 80 Ω cm^2. In particular, hCMEC/D3 cell monolayers expressed TEER values of 72 ± 9.5 Ω cm^2, HRPE cell monolayers expressed TEER values of 60 ± 2.5 Ω cm^2 and IEC-6 cell monolayers showed TEER values of 69 ± 6.5 Ω cm^2, when each cell line was grown separately from the others at its specific cell density in its own growth medium in blocks sharing the same CELLBLOKS® channel, as illustrated in figure 4.

As complementary validation of the barrier integrity of cell monolayers developed in CELLBLOKS®, the immunofluorescence staining and imaging of the tight junctions proteins ZO-1 and occludin was performed when TEER values rise to a plateau, indicating the establishment of a fully functional cell barrier [13]. ZO-1 and occludin are extensively investigated junctional complexes [14, 15], therefore these proteins were selected to be localized within 12 day-cultured hCMEC/D3, 8-day-cultured IEC-6, and 8-day-cultured HRPE cell monolayers. Figure S1(A) shows that immunofluorescence staining of ZO-1

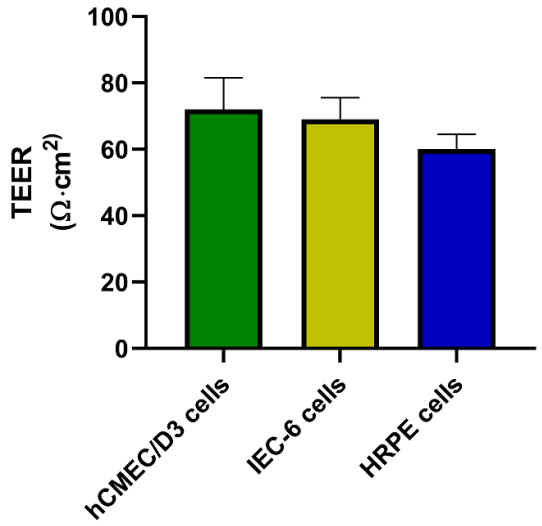

Figure 4. Tightness of the different cell monolayers based on the TEER values using chopstick electrodes linked to the Millicell voltmeter. Each histogram represents the mean ± SEM of three independent experiments, run in duplicate. There are no significant differences among the mean values of the three types of cell monolayers (one-way ANOVA followed by Tukey's multiple comparison test) after 12 culture-days for hCMEC/D3 cells and 8 culture-days for IEC-6 cells and HRPE cells, respectively.

protein was an appreciable strand along the membrane of all the three types of cell layers, aligning with their TEER values. Occludin was also found to be expressed in all the three types of cell layers (figure S1(B)). Overall, the immunostaining suggests expression of the investigated tight junction markers.

Non-specific staining controls were additionally carried out using only fluorescent secondary antibodies, indicating the lack of green or red staining in tight junctions in the absence of primary antibodies (figures S1(A) and (B)).

Overall, the results described in this section demonstrated that well-established junction proteins staining were obtained on the cell monolayers developed in CELLBLOKS® systems.

3.2. Simulation in CELLBLOKS® platform of IVA and OA of eugenol or celiprolol to study their permeation across intestinal, endothelial and choroidal cell barriers

In the present study, the CELLBLOKS® platform is proposed for the first time to perform *in vitro* studies combining intestinal permeability with subsequent BBB and BCSFB permeability through distribution measurements and comparing IVA with OA in parallel. In this study two molecules were chosen as prototypes: eugenol as test compound, being known for its high aptitude to penetrate in the CNS from the bloodstream [3], and celiprolol as negative control, known for its poor ability to permeate in the CNS from the bloodstream, being a substrate of the efflux transporter P-gp [7]. The concentrations of the tested compounds reaching each compartment *in vitro* at specific time points were evaluated by HPLC analysis.

In our *in vitro* system, IVA was therefore simulated using two configurations of the CELLBLOKS® system: one in the presence of the IB, as represented in figure 3(A), and another one by excluding the IB, as represented in figure 3(B). Both the configurations were used by adding 7.5 μM test compound (celiprolol or eugenol) directly to the bloodstream-mimetic channel of CELLBLOKS® platform, facing the apical side of the BBB and the basolateral side of the BCSFB, respectively, and representing therefore their donor compartment of each single compound. The use of the two configurations was adopted in the aim to verify the potential ability of the IB to influence the drug permeation in the CNS. OA was instead simulated with the CELLBLOKS® configuration reported in figure 3(C) by adding each test compound at a final concentration of 25 μM to the apical (luminal) compartment of IB-mimetic rat IEC-6 cell monolayers. The absorption of the compounds in the mimicked-systemic circulation was measured in the basolateral compartment. Moreover, the compounds were quantified in both BBB-delimited neuronal- like receiver compartment and BCSFB-delimited receiver compartment after their simulated IVA and OA in the CELLBLOKS® platform. The compounds were incubated up to 2 h. The TEER values of each monolayer monitored before the incubation with celiprolol or eugenol did not appear statistically different with respect to the TEER values measured after 2 h of incubation, indicating that the chosen concentrations of the compounds did not alter the integrity of the monolayers. Finally, the permeations of celiprolol or eugenol in the receiver compartments were evaluated by comparing their crossing ability of both the cell-free filters and the filters where cell monolayers were grown and differentiated to obtain the simulated IB, BBB, and BCSFB.

3.3. Simulated IVA of celiprolol

Figure 5(A) reports a comparison of simulated IVA of celipropol between the configuration of the CELLBLOKS® system with cell-free filters and the configuration in the presence of IB, BBB, and BCSFB (described in figure 3(A)). In particular, the concentrations of celiprolol in the central-mimicking receiver compartment of the cell-free filter were 0.65 ± 0.01 μM and 1.28 ± 0.03 μM, respectively, 60 and 120 min after its addition (7.5 μM final concentration at time zero) in the bloodstream-mimetic channel of CELLBLOKS® platform (simulation of IVA). At the same time, the celiprolol concentrations in the donor compartment were 5.24 ± 0.06 μM and 4.71 ± 0.09 μM, respectively (table 1). Based on these data, the receiver recovery ratio (R/D ratio) values of celiprolol crossing the cell-free filters were calculated as the ratio between its concentration in the receiver (R) compartment and in the donor (D) compartment

(R/D) at the same time points, obtaining the following values: 0.124 ± 0.002 at 60 min and 0.272 ± 0.008 at 120 min (table 1). On the other hand, the presence of the IB, BBB, and BCSFB like cell monolayers on the filters induced a drastic decrease ($P < 0.0001$) of celiprolol permeation in the receiving compartments of CELLBLOKS® platform. In particular, the concentrations of this compounds in the bloodstream-mimetic channel of CELLBLOKS® platform were almost the same as detected in the system without cell monolayers (5.06 ± 0.36 μM and 4.92 ± 0.38 μM at 60 and 120 min, respectively, as reported in table 1), whereas in the BBB receiving compartment the celiprolol concentrations were 0.20 ± 0.03 μM at 60 min and 0.40 ± 0.07 μM at 120 min, or 0.18 ± 0.01 μM at 60 min and 0.43 ± 0.03 μM at 120 min in the BCSFB receiving compartment (table 1). In this case, the R/D ratio values of celiprolol crossing the BBB and BCSFB filters were 0.039 ± 0.006 at 60 min and 0.081 ± 0.016 at 120 min for the BBB filters or 0.035 ± 0.003 at 60 min and 0.087 ± 0.009 at 120 min for the BCSFB filters (table 1).

These results indicate that the BBB- and BCSFB-like cell monolayers are efficacious in simulating the physiological barriers between the bloodstream and the CNS. Indeed, the presence of cell monolayers significantly reduced ($P < 0.0001$) the celiprolol permeation across the filters between the bloodstream-mimetic channel of CELLBLOKS® platform and the receiving central-mimetic compartments, allowing to decrease up to 70% its R/D ratio value after two hours of incubation, in comparison to the permeation across the filters without cell monolayers.

In this case, also the IB-like monolayer appeared as an efficient barrier between the bloodstream and the intestinal lumen. Indeed, the celiprolol concentrations in the IB receiving compartment were 0.15 ± 0.01 μM and 0.35 ± 0.02 μM at 60 and 120 min, allowing to obtain R/D ratio values of 0.029 ± 0.003 and 0.070 ± 0.007, respectively (table 1). According to these data, the reduction of celiprolol permeation across the filters in the presence of IB can be quantified by a decrease of R/D ratio of 74%, after two hours of incubation.

Table 1 reports also the results obtained by the IVA simulation of celiprolol using the CELLBLOKS® configuration obtained in the absence of IB which is represented in figure 3(B). It can be observed that the absence of the IB does not qualitatively change the ability of the BBB and BCSFB like monolayers to counteract the celiprolol permeation to their receiving compartments, as reported in figure S2.

3.4. Simulated OA of celiprolol

OA of celiprolol was simulated by adding it to the apical (or luminal) compartment mimicking the intestinal lumen (25 μM final concentration) and measuring its permeation to the basolateral compartment mimicking the bloodstream; then, the ability of celiprolol to permeate in the BBB- and BCSFB-like receiver compartments was further evaluated. As above described, all these measurements were performed both in the absence (cell-free filters) and in the presence of cell monolayers.

In figure 5(B) it is evidenced that in the absence of cell monolayers, the celiprolol concentrations detected in the bloodstream-like compartment were

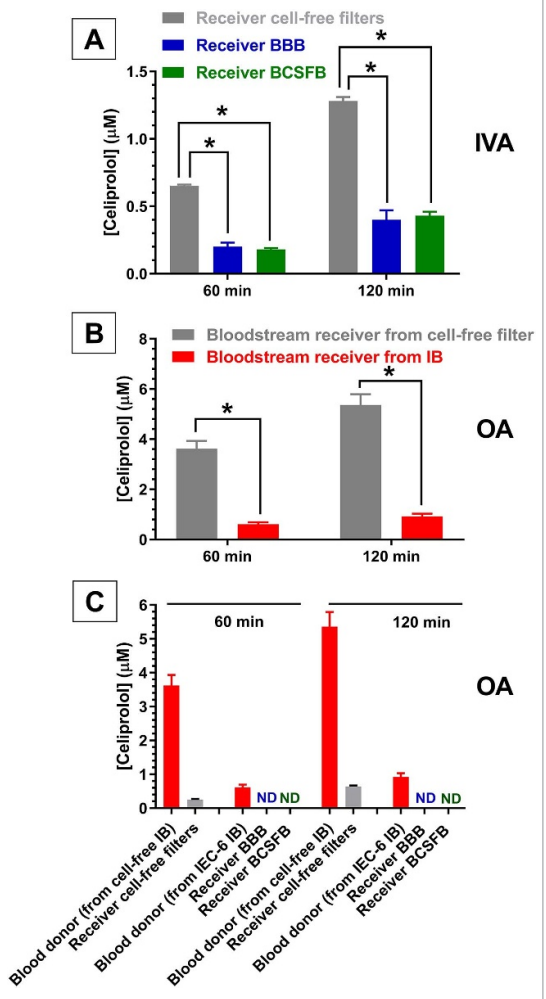

Figure 5. Simulation of intravenous (IVA) or oral (OA) administrations of celiprolol and its permeation in the CNS using the CELLBLOKS® platform with the configuration obtained in the presence of IB. (A) Concentrations of celiprolol in the receiving compartments mimicking the brain parenchyma (receiver BBB) or the CSF (receiver BCSFB) 60 min and 120 min after its introduction in the bloodstream-mimetic channel (7.5 μM final concentration, simulated IVA). The same measurements were performed also in the absence of cell monolayers (receiver-cell free filters) mimicking the BBB and BCSFB. (B) Concentrations of celiprolol in the bloodstream-mimetic channel (bloodstream receiver from IB) 60 min and 120 min after its introduction in the apical compartment mimicking the intestinal lumen (25 μM final concentration, simulated OA). The same measurements were performed also in the absence of cell monolayers (bloodstream receiver from cell-free filters). (C) Celiprolol concentrations in the central-mimicking compartments (receiver BBB or receiver BCSFB) after permeation from the blood donor mimicking channel reached after simulated OA. The same measurements were performed also in the absence of cell monolayers. Data are expressed as the mean ± SEM of four independent experiments ($n = 4$). *$P < 0.0001$; ND = no detected.

3.62 ± 0.31 μM and 5.36 ± 0.43 μM at 60 and 120 min, respectively, whereas in the presence of IEC-6 cell monolayer the concentrations were 0.60 ± 0.08 μM and 0.92 ± 0.11 μM, respectively (table 2). In this case, the corresponding R/D ratio values decreased from 0.196 ± 0.021 and 0.321 ± 0.032 (cell-free filters) at 60 and 120 min, respectively, to 0.033 ± 0.007 and 0.049 ± 0.009 (filters with IEC-6 monolayers) (table 2). These data indicate that the IB like cell monolayer was efficacious in simulating the physiological barriers between the intestinal lumen and the bloodstream, being its presence able to significantly reduce ($P < 0.0001$) the permeation of celiprolol across the filter of the CELLBLOKS® platform, evidencing a decrease of the R/D ratio value of about the 85%.

The configuration of CELLBLOKS® system built in the absence of cell monolayers allowed to evidence that celiprolol not only reached the bloodstream-like donor channel after its simulated OA (as above described), but it was also able to permeate and achieve measurable concentrations in cell-free filters receiver compartment mimicking the CNS, after both 60 min and 120 min (figure 5(C)) reaching the values of 0.25 ± 0.02 μM and 0.64 ± 0.03 μM, respectively (table 2). In this case, the corresponding R/D ratio values were calculated as 0.070 ± 0.008 and 0.119 ± 0.011, respectively (table 2). The configuration of CELLBLOKS® system built in the presence of cell monolayers was used to evaluate the ability of celiprolol to permeate in the mimicking BBB and BCSFB receiving compartments after its simulated OA. At these conditions, celiprolol was able to reach the bloodstream-like donor channel, as above described, but it appeared undetectable in the BBB- and BCSFB-delimited receiver compartments after 60 min and 120 min of the simulated OA (figure 5(C)), indicating its inability to reach the central compartments, where the R/D ratio values were zero (table 2). Therefore, the results of the permeations obtained in the presence of the IB-, BBB- and BCSFB-like cell monolayers in the CELLBLOKS® platform became crucial to recognize *in vitro* the inability of celiprolol to reach the CNS normally observed *in vivo* after its OA [16].

3.5. Simulated IVA of eugenol

Figure 6(A) reports a comparison of simulated IVA of eugenol between the configuration of the CELLBLOKS® system with cell-free filters and the configuration in the presence of IB, BBB, and BCSFB (described in figure 3(A)). In particular, the concentrations of eugenol in the central-mimicking receiver compartment of the cell-free filter were 0.56 ± 0.03 μM and 0.92 ± 0.04 μM, respectively, 60 and 120 min after its addition (7.5 μM final concentration at time zero) in the bloodstream-mimetic channel of CELLBLOKS® platform (simulation of IVA). At the same times, the eugenol concentrations in the donor compartment were 5.00 ± 0.40 μM and 3.85 ± 0.07 μM, respectively, allowing to obtain the R/D ratio values of 0.112 ± 0.011 at 60 min and 0.239 ± 0.011 at 120 min, which were not significantly different from the corresponding celiprolol ones, as reported in table 1.

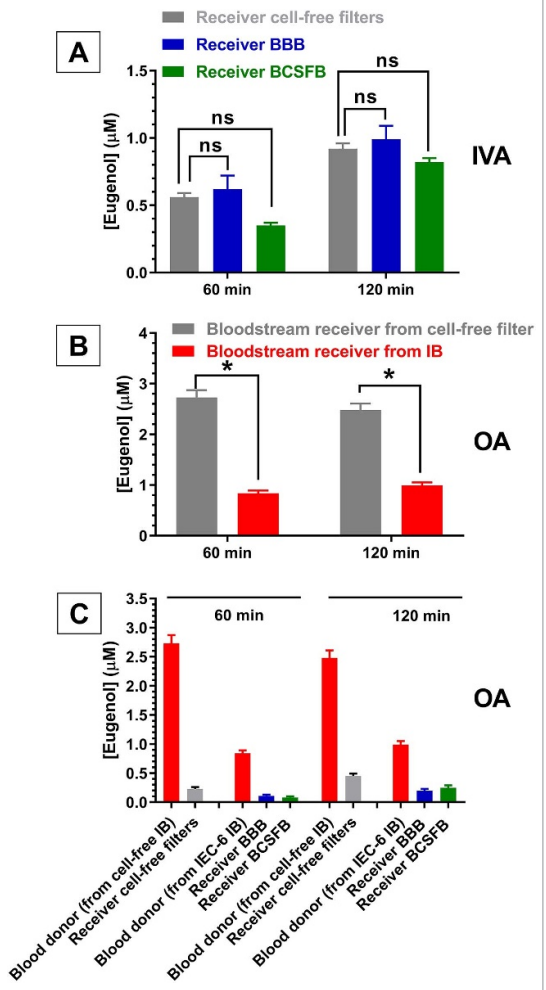

Figure 6. Simulation of intravenous (IVA) or oral (OA) administrations of eugenol and its permeation in the CNS using the CELLBLOKS® platform with the configuration obtained in the presence of IB. (A) Concentrations of eugenol in the receiving compartments mimicking the brain parenchyma (receiver BBB) or the CSF (receiver BCSFB) 60 min and 120 min after its introduction in the bloodstream-mimetic channel (7.5 μM final concentration, simulated IVA). The same measurements were performed also in the absence of cell monolayers (receiver cell-free filters) mimicking the BBB and BCSFB. (B) Concentrations of eugenol in the bloodstream-mimetic channel (bloodstream receiver from IB) 60 min and 120 min after its introduction in the apical compartment mimicking the intestinal lumen (25 μM final concentration, simulated OA). The same measurements were performed also in the absence of cell monolayers (bloodstream receiver from cell-free filter). (C) Eugenol concentrations in the central-mimicking compartments (receiver BBB or receiver BCSFB) after permeation from the blood donor mimicking channel reached after simulated OA. The same measurements were performed also in the absence of cell monolayers. Data are expressed as the mean ± SEM of four independent experiments ($n = 4$). *$P < 0.0001$.

The presence of the BBB and BCSFB-like cell monolayers on the filters did not induce a decrease

of the eugenol permeation in the receiving compartments of CELLBLOKS® platform (figure 6(A)), differently from what was described for celiprolol (figure 5(A)). In particular, the eugenol concentrations in the BBB receiving compartments were 0.62 ± 0.10 μM at 60 min and 0.99 ± 0.10 μM at 120 min, or 0.35 ± 0.02 μM at 60 min and 0.82 ± 0.03 μM at 120 min in the BCSFB receiving compartment (table 1). Based on these data, the R/D ratio values of eugenol crossing the BBB and BCSFB filters were 0.114 ± 0.018 at 60 min and 0.224 ± 0.024 at 120 min for the BBB filters, or 0.064 ± 0.004 at 60 min and 0.186 ± 0.010 at 120 min for the BCSFB filters (table 1).

As evidenced in figure 6(A), the concentrations of eugenol in the BBB or BCSFB receiving compartments were not significantly different after its permeation across the cell-free filters or the filters with the cell monolayers. This result indicates that the BBB and BCSFB mimetic monolayers do not constitute barriers for the eugenol permeation and this behaviour appears completely different compared to that of celiprolol. Indeed, as evidenced in figure 7, the R/D ratio values related to the eugenol permeation across the filters without cell monolayers were not significantly changed by the presence of the BBB- or BCSFB-mimicking cell monolayers, whereas in the case of celiprolol the R/D ratio values were significantly lowered.

On the other hand, the IB-like monolayer appeared as an efficient barrier for eugenol between the bloodstream and the intestinal lumen. Indeed, the concentrations of this compound in the IB receiving compartment were 0.17 ± 0.01 μM and 0.29 ± 0.01 μM at 60 and 120 min, allowing to obtain R/D ratio values of 0.032 ± 0.001 and 0.066 ± 0.001, respectively (table 1). According to these data, the reduction of eugenol permeation across the filters in the presence of IB can be quantified by a decrease of R/D ratio of 72%, after two hours of incubation.

Table 1 reports also the results obtained by the IVA simulation of eugenol using the CELLBLOKS® configuration obtained in the absence of IB which is represented in figure 3(B). It can be observed that the absence of the IB does not qualitatively change the aptitude of the BBB and BCSFB like monolayers to allow the eugenol permeation to their receiving compartments, as reported in figure S3.

3.6. Simulated OA of eugenol

OA of eugenol was simulated by its adding to the gut mimetic apical (or luminal) compartment delimited by IEC-6 cell monolayer (25 μM final concentration) and measuring its permeation to the bloodstream-like basolateral compartment; then, the ability of eugenol to permeate into the BBB and BCSFB mimetic receiver compartments was further

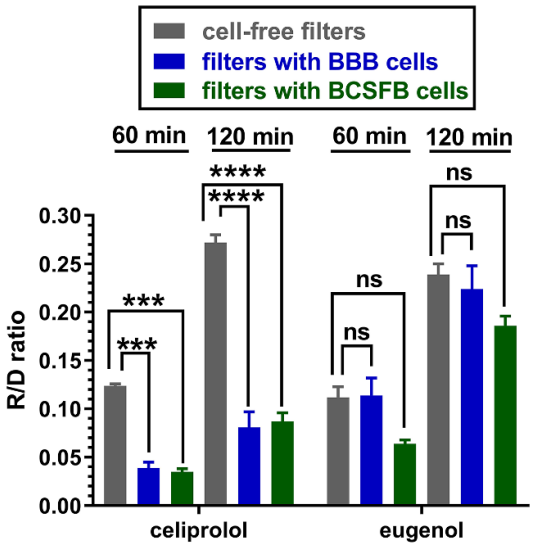

Figure 7. Simulation of intravenous administration (IVA) of celiprolol or eugenol and their permeation in the CNS in the CELLBLOKS® platform: receiver recovery ratio (R/D ratio) values of each compound between receiving compartments mimicking the brain parenchyma (defined by filters with BBB cells) or the CSF (defined by filters with BCSFB cells) and the bloodstream-mimetic channel. The same measurements were performed also in the absence of cell monolayers (cell-free filters) mimicking the BBB and BCSFB. Data are expressed as the mean ± SEM of four independent experiments. *** $P < 0.001$; **** $P < 0.0001$; ns = no significant difference.

evaluated. As above described, all these measurements were performed both in the absence (cell-free filters) and in the presence of cell monolayers.

Figure 6(B) evidences that in the absence of cell monolayers, the eugenol concentrations detected in the mimicking bloodstream compartment were 2.73 ± 0.14 μM and 2.48 ± 0.13 μM at 60 and 120 min, respectively, whereas in the presence of IEC-6 cell monolayer the concentrations were 0.84 ± 0.05 μM and 0.99 ± 0.06 μM, respectively (table 2). In this case, the corresponding R/D ratio values decreased from 0.187 ± 0.010 and 0.287 ± 0.015 (cell-free filters) at 60 and 120 min, respectively, to 0.039 ± 0.003 and 0.064 ± 0.005 (filters with IEC-6 monolayers) (table 2). These data indicate that the IB-like cell monolayer is efficacious in simulating the physiological barriers between the intestinal lumen and the bloodstream, being its presence able to significantly reduce ($P < 0.0001$) the permeation of eugenol across the filter of the CELLBLOKS® platform, evidencing a decrease of the R/D ratio value of about the 79%.

The configuration of CELLBLOKS® system built in the absence of cell monolayers allowed to evidence that eugenol not only reached the bloodstream-like donor channel after its simulated OA (as above described), but it was also able to permeate and achieve measurable concentrations in cell-free filters

Table 1. Simulation of intravenous administration (IVA) of celiprolol or eugenol and their permeation in the CNS across BBB or BSCFB by using the CELLBLOKS® system assembled in the presence or in the absence of IEC-6 simulating the intestinal barrier IB): the concentrations (μM) of each compound were detected in the donor compartment 'D' (bloodstream-mimetic channel of CELLBLOKS® platform) and in the receiver compartments 'R' mimicking the intestinal lumen (IB), the CSF (BCSFB) or the brain parenchyma (BBB) at 0, 60, and 120 min following their incubation of 7.5 μM in the bloodstream-mimetic channel. The measurements were also performed in the complete absence (cell-free filters) of the cell monolayers mimicking the IB, BBB or BCSFB. For each condition evaluated, the receiver recovery ratio (R/D ratio) values are reported. Data are expressed as the mean ± SEM of four independent experiments ($n = 4$).

Celiprolol, IVA simulation							
		CELLBLOKS® system assembled in the presence of IB			CELLBLOKS® system assembled in the absence of IB		CELLBLOKS® system assembled in the complete absence of cells
	Time (min)	Filters with IB	Filters with BBB	Filters with BCSFB	Filters with BBB	Filters with BCSFB	BBB, BCSFB or IB cell-free filters
Receiving (R)	0	0 μM	0 μM	0 μM	0 μM	0 μM	0 μM
	60	0.15 ± 0.01 μM	0.20 ± 0.03 μM	0.18 ± 0.01 μM	0.31 ± 0.01 μM	0.18 ± 0.01 μM	0.65 ± 0.01 μM
	120	0.35 ± 0.02 μM	0.40 ± 0.07 μM	0.43 ± 0.03 μM	0.42 ± 0.04 μM	0.31 ± 0.01 μM	1.28 ± 0.03 μM
Donor (D)	0	7.50 ± 0.16 μM	7.50 ± 0.16 μM	7.50 ± 0.16 μM	7.50 ± 0.12 μM	7.50 ± 0.12 μM	7.50 ± 0.12 μM
	60	5.06 ± 0.36 μM	5.06 ± 0.36 μM	5.06 ± 0.36 μM	5.24 ± 0.11 μM	5.24 ± 0.11 μM	5.24 ± 0.06 μM
	120	4.92 ± 0.38 μM	4.92 ± 0.38 μM	4.92 ± 0.38 μM	4.75 ± 0.15 μM	4.75 ± 0.15 μM	4.71 ± 0.09 μM
Ratio (R/D)	0	0	0	0	0	0	0
	60	0.029 ± 0.003	0.039 ± 0.006	0.035 ± 0.003	0.059 ± 0.002	0.034 ± 0.002	0.124 ± 0.002[a]
	120	0.070 ± 0.007	0.081 ± 0.016	0.087 ± 0.009	0.088 ± 0.009	0.066 ± 0.003	0.272 ± 0.008[b]
Eugenol, IVA simulation							
		CELLBLOKS® system assembled in the presence of IB			CELLBLOKS® system assembled in the absence of IB		CELLBLOKS® system assembled in the complete absence of cells
	Time (min)	Filters with IB	Filters with BBB	Filters with BCSFB	Filters with BBB	Filters with BCSFB	BBB, BCSFB or IB cell-free filters
Receiving (R)	0	0 μM	0 μM	0 μM	0 μM	0 μM	0 μM
	60	0.17 ± 0.01 μM	0.62 ± 0.10 μM	0.35 ± 0.02 μM	0.55 ± 0.05 μM	0.35 ± 0.04 μM	0.56 ± 0.03 μM
	120	0.29 ± 0.01 μM	0.99 ± 0.10 μM	0.82 ± 0.03 μM	0.89 ± 0.08 μM	0.75 ± 0.04 μM	0.92 ± 0.04 μM
Donor (D)	0	7.50 ± 0.11 μM	7.50 ± 0.11 μM	7.50 ± 0.11 μM	7.50 ± 0.09 μM	7.50 ± 0.09 μM	7.50 ± 0.11 μM
	60	5.46 ± 0.21 μM	5.46 ± 0.21 μM	5.46 ± 0.21 μM	4.82 ± 0.63 μM	4.82 ± 0.63 μM	5.00 ± 0.40 μM
	120	4.40 ± 0.08 μM	4.40 ± 0.08 μM	4.40 ± 0.08 μM	3.79 ± 0.04 μM	3.79 ± 0.04 μM	3.85 ± 0.07 μM
Ratio (R/D)	0	0	0	0	0	0	0
	60	0.032 ± 0.001	0.114 ± 0.018	0.064 ± 0.004	0.114 ± 0.018	0.072 ± 0.013	0.112 ± 0.011[a]
	120	0.066 ± 0.001	0.224 ± 0.024	0.186 ± 0.010	0.234 ± 0.021	0.198 ± 0.011	0.239 ± 0.011[b]

[a] Values not significantly different from each other ($P > 0.05$).

[b] Values not significantly different from each other ($P > 0.05$).

Table 2. Simulation of oral administration (OA) of celiprolol or eugenol considering their permeation across the IB and then across BBB or BSCFB. In the CELLBLOKS® platform the IB separates the mimicked intestinal lumen (Donor compartment 'D') from the bloodstream-mimetic channel (Receiving compartment 'R'); the BBB separates the mimicked brain parenchyma (Receiving compartment 'R') from the bloodstream-mimetic channel (in this case Donor Compartment 'D'); the BCSFB separates the mimicked CSF (Receiving compartment 'R') from the bloodstream-mimetic channel (in this case Donor Compartment 'D'). The measurements were performed in the absence (cell-free filters) and in the presence of the cell monolayers mimicking the IB, BBB or BCSFB. For each condition evaluated, the receiver recovery ratio (R/D ratio) values are reported. Data are expressed as the mean ± SEM of four independent experiments ($n = 4$).

Celiprolol, OA			
CELLBLOKS® systems assembled without cell monolayers (cell-free filters)			
	Time (min)	IB cell-free filters	BBB or BCSFB cell-free filters
Receiving compartment (R)	0	0 μM	0 μM
	60	3.62 ± 0.31 μM	0.25 ± 0.02 μM
	120	5.36 ± 0.43 μM	0.64 ± 0.03 μM
Donor compartment (D)	0	25.00 ± 0.19 μM	0 μM
	60	18.42 ± 1.10 μM	3.62 ± 0.31 μM
	120	16.73 ± 0.96 μM	5.36 ± 0.43 μM
Ratio (R/D)	0	0	—
	60	0.196 ± 0.021	0.070 ± 0.008
	120	0.321 ± 0.032	0.119 ± 0.011

Celiprolol, OA				
CELLBLOKS® systems assembled with cell monolayers (filters with cells)				
	Time (min)	Filters with IB	Filters with BBB	Filters with BCSFB
Receiving compartment (R)	0	0 μM	0 μM	0 μM
	60	0.61 ± 0.08 μM	0 μM	0 μM
	120	0.92 ± 0.11 μM	0 μM	0 μM
Donor compartment (D)	0	25.00 ± 0.13 μM	0 μM	0 μM
	60	18.05 ± 1.93 μM	0.61 ± 0.08 μM	0.61 ± 0.08 μM
	120	18.65 ± 1.30 μM	0.92 ± 0.11 μM	0.92 ± 0.11 μM

(Continued.)

Table 2. (Continued.)

Ratio (R/D)	0	0	—	—
	60	0.033 ± 0.007	0	0
	120	0.049 ± 0.009	0	0
Eugenol, OA				
CELLBLOKS® systems assembled without cell monolayers (cell-free filters)				
	Time (min)	IB cell-free filters	BBB or BCSFB cell free filters	
Receiving compartment (R)	0	0 μM	0 μM	
	60	2.73 ± 0.14 μM	0.23 ± 0.03 μM	
	120	2.48 ± 0.13 μM	0.45 ± 0.04 μM	
Donor compartment (D)	0	25.00 ± 0.17 μM	0 μM	
	60	14.61 ± 0.08 μM	2.73 ± 0.14 μM	
	120	8.63 ± 0.05 μM	2.48 ± 0.13 μM	
Ratio (R/D)	0	0	—	
	60	0.187 ± 0.010	0.085 ± 0.012	
	120	0.287 ± 0.015	0.180 ± 0.019	
Eugenol, OA				
CELLBLOKS® systems assembled with cell monolayers (filters with cells)				
	Time (min)	Filters with IB	Filters with BBB	Filters with BCSFB
Receiving compartment (R)	0	0 μM	0 μM	0 μM
	60	0.84 ± 0.05 μM	0.11 ± 0.02 μM	0.10 ± 0.02 μM
	120	0.99 ± 0.06 μM	0.20 ± 0.03 μM	0.25 ± 0.04 μM
Donor compartment (D)	0	25.00 ± 0.15 μM	0 μM	0 μM
	60	21.47 ± 0.93 μM	0.84 ± 0.05 μM	0.84 ± 0.05 μM
	120	15.59 ± 0.72 μM	0.99 ± 0.06 μM	0.99 ± 0.06 μM
Ratio (R/D)	0	0	—	—
	60	0.039 ± 0.003	0.126 ± 0.026	0.093 ± 0.025
	120	0.064 ± 0.005	0.203 ± 0.033	0.253 ± 0.043

receiver compartment mimicking the CNS, after both 60 min and 120 min (figure 6(C)) reaching the values of 0.23 ± 0.03 μM and 0.45 ± 0.04 μM, respectively (table 2). In this case, the corresponding R/D ratio values were calculated as 0.085 ± 0.012 and 0.180 ± 0.019, respectively (table 2). The configuration of CELLBLOKS® system built in the presence of cell monolayers was used to evaluate the ability of eugenol to permeate in the mimicking BBB and BCSFB receiving compartments after its simulated OA. At these conditions, eugenol was able to reach the bloodstream-like donor channel, as above described; moreover, differently from celiprolol, its further ability to permeate in the BBB- and BCSFB-delimited receiver compartments appeared not counteracted by the presence of the cell monolayers. Indeed, the eugenol concentrations in the BBB receiving compartments were 0.11 ± 0.02 μM at 60 min and 0.20 ± 0.03 μM at 120 min, or 0.10 ± 0.02 μM at 60 min and 0.25 ± 0.04 μM at 120 min in the BCSFB receiving compartment (table 2). In this case, the R/D ratio values of eugenol crossing the BBB and BCSFB filters were 0.126 ± 0.026 at 60 min and 0.203 ± 0.033 at 120 min for the BBB filters, or 0.093 ± 0.025 at 60 min and 0.253 ± 0.043 at 120 min for the BCSFB filters (table 2). These data confirm the marked ability of eugenol to penetrate in central compartments from the bloodstream mimetic channel in comparison to celiprolol, whose ability at the same conditions was zero.

3.7. Dopaminergic neuron-like PC12 cells were induced to release DA by eugenol crossing BBB and BCSFB

A further experimental approach combining CELLBLOKS® and NANOSTACKS™ was designed to test whether eugenol, after crossing the brain barriers via simulated IVA or OA, could reach the effective concentration to elicit dopaminergic neuronal activity in terms of DA release in neuron-like compartments.

To this end, brain dopaminergic networks were mimicked by growing differentiated PC12 cells for 14 d into neuronal-like cells on NANOSTACKS™ inserts with 100 ng ml^{-1} NGF and subsequently placed inside the blocks delimited by the BBB and BCSFB immediately prior to the beginning of permeation experiments, where eugenol was added directly in the bloodstream-like channel for simulated IVA (7.5 μM final concentration) or in the apical side of IB for simulated OA (25 μM final concentration), as described above. Indeed, as shown in figure 8, in both IVA and OA simulated conditions, eugenol reached a concentration suitable to evoke a DA release from neuron-like differentiated PC12 cells on NANOSTACKS™ inserts (figure 8(A)), both at 60 min and 120 min after crossing the BBB and BCSFB and accumulating into the respective compartments (figure 8(B)).

In the IVA simulated conditions, eugenol reached a concentration of 0.55 ± 0.05 μM after 60 min and 0.89 ± 0.08 μM after 120 min in the BBB-delimited compartment (figure 8(B)), inducing a DA release of 1200 ± 12 pg ml^{-1} and 7839 ± 126 pg ml^{-1}, respectively, from PC12 cells (figure 8(A)). It should be noted that while the eugenol concentration nearly doubled when the permeation period was extended from 60 to 120 min ($P < 0.001$; figure 8(B), the corresponding DA release increased approximately 6.5-fold ($P < 0.0001$; figure 8(A)). A similar result was observed in the BCSFB-delimited compartment, where eugenol reached a concentration of 0.35 ± 0.04 μM after 60 min of incubation and increased to 0.75 ± 0.04 μM after 120 min, showing nearly two-fold increase ($P < 0.0001$; figure 8(B); the corresponding DA release was quantified as 1958 ± 174 pg ml^{-1} at 60 min and then increased to 7922 ± 434 pg ml^{-1} at 120 min, indicating an approximately four-fold increase ($P < 0.0001$; figure 8(A)). Furthermore, no statistical differences were observed between the eugenol concentrations reached in the BBB- and BCSFB-delimited compartments at the same incubation time (60 min or 120 min) (figure 8(B), and the same result was reflected in the DA release from PC12 cells on NANOSTACKS™ inserts placed in the same compartments (figure 8(A)).

In OA simulated conditions, eugenol reached a concentration of 0.11 ± 0.02 μM after 60 min of incubation and 0.20 ± 0.03 μM after 120 min in the BBB-delimited compartment (figure 8(B)), inducing a DA release of 1458 ± 235 pg ml^{-1} and 8734 ± 172 pg ml^{-1}, respectively, from PC12 cells (figure 8(A)). Although no statistically significant differences in eugenol concentrations were observed between 60 min and 120 min of incubation (figure 8(B)), the corresponding DA release from PC12 cells increased approximately 6-fold ($P < 0.0001$; figure 8(A)). A similar result was observed in the BCSFB-delimited compartment, where no statistically significant differences in eugenol concentrations were observed between 60 min and 120 min of incubation, with values corresponding to 0.08 ± 0.02 μM and 0.25 ± 0.04 μM, respectively (figure 8(B), whereas the corresponding DA release from PC12 cells was quantified at 1231 ± 41 pg ml^{-1} at 60 min and 7913 ± 418 pg ml^{-1} at 120 min, indicating a six-fold increase ($P < 0.0001$; figure 8(A)).

As observed in IVA simulated conditions, the eugenol concentrations reached in the BBB- and BCSFB-delimited compartments were not statistically significant different at the same incubation time of 60 min or 120 min (figure 8(B), and the same result was displayed as DA release from PC12 cells placed in the same compartments (figure 8(A)).

Finally, the baseline DA release values at 60 min (509 ± 58 pg ml^{-1}) and 120 min (683 ± 123 pg ml^{-1})

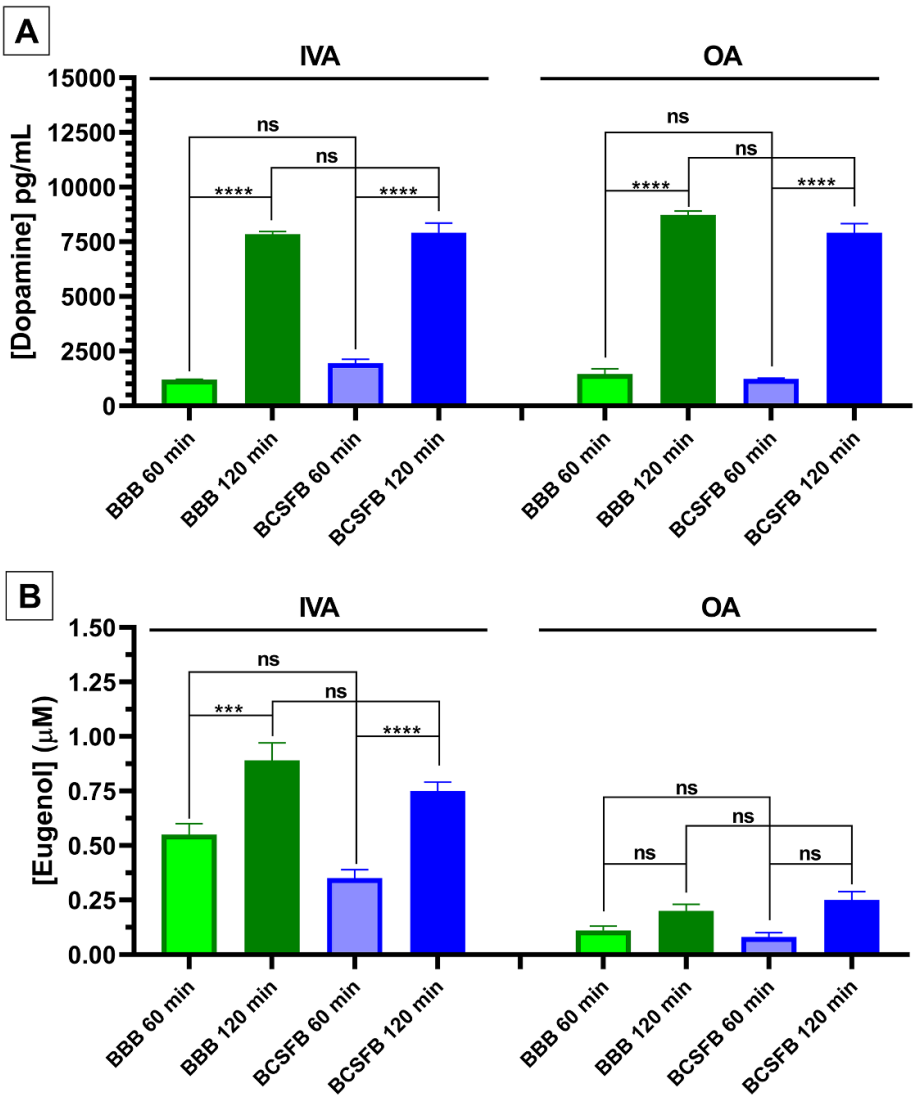

Figure 8. Time-dependence of eugenol-induced dopamine release from PC12 cells in NANOSTACKS™. (A) DA released by PC12 cells inside the BBB- and BCSFB-delimited neuronal-like compartments and stimulated by eugenol following a simulated IVA (7.5 μM in the bloodstream-like channel) or OA (25 μM in the apical side of IB) after 60- and 120 min. (B) Corresponding eugenol concentrations, reached after 60 and 120 min in the BBB- and BCSFB-delimited neuronal compartments, that induced DA release. In both (A) and (B) plots, data were expressed as mean $\pm$ SEM of $n = 4$ independent measures and analysed by two-way ANOVA, followed by Tukey's multiple comparisons test. $^{***}P < 0.001$; $^{****}P < 0.0001$; ns: not significant.

were significantly lower ($P < 0.05$) than the corresponding eugenol-induced DA release values from PC12 cells, showed in figure 8(A). Although a slight increase in baseline DA release was observed at 120 min compared to 60 min, the two values were not statistically different from each other. Therefore, a not significant contribution of baseline to the stimulation of eugenol-induced DA release from PC12 cells was observed.

4. Discussion

The design of cell-based models is currently required for *in vitro* studies aimed to predict the intestinal permeability of potential new drugs and their potential ability to permeate in the CNS. The availability of this type of models can allow, indeed, to reduce the use of animal models when studying the ability of potential new neuroactive drugs to target their therapeutic site.

In this context, the ability to engineer compartment permeability is critical for *in vitro* systems to achieve sustainability, robustness, and complexity, considering that biological compartments delimited by physiological barriers rely on dynamically controlled permeability for substance exchange and complex cellular activities. The design of *in vitro* compartments with these characteristics is therefore considered a challenge [17, 18]. Recently, a microfluidic platform has been proposed by Xavier and co-workers as a robust *in vitro* model for studies related to OA of new compounds, in particular for their bioaccessibility and intestinal permeability [18].

CELLBLOKS®, a new MPS developed and patented by Revivocell, is here proposed for the first

time to perform *in vitro* studies combining intestinal permeability with subsequent BBB and BCSFB permeability of model compounds through systemic distribution measurements and comparing IVA with OA in parallel. This platform is suitable for creating pre-established combinations of appropriate cell monolayers *in vitro* simulating several physiological barriers that protect and restrict specific microenvironments, such as the brain parenchyma, the CSF, the intestinal lumen or the bloodstream, while allowing the selective exchange of substances between them, exactly as it occurs in the body.

Although primary human cerebral microvessel endothelial cells would ideally be the model of choice for BBB *in vitro*, the poor availability of fresh human brain non-tumoral tissue makes them useless. Therefore, in our study, the hCMEC/D3 cell line was used as well recognized cell model of the human BBB suitable for molecular studies on drug transport mechanisms with relevance to the CNS [19].

HRPE cell line was chosen as *in vitro* model of choroid plexus epithelium (CPE), since high level of morphological and functional correspondence between these neuro-epithelia has been extensively demonstrated [11, 12, 20, 21]. Therefore, we utilized established HRPE cell line as easier to be retrieved and cultured than primary human CPE cells, taking also into account that there is no evidence indicating availability of a primary or immortalized cell culture of pathologically unaltered human CPE [22, 23].

In order to simulate the IB in the CELLBLOKS® system, we have firstly considered the properties of two human cellular lines, Caco and human intestinal epithelial cells (HIEC), potentially available for *in vitro* permeation studies. Caco cell lines have a colonic cancerous origin, inducing in the cell monolayers structural and functional features different than those of small bowel cells. In particular, higher TEER values (due to stronger tight junctions) are known to cause *in vitro* systematic underestimations of drug paracellular diffusion kinetics; moreover, altered expression of transporters and enzymes does not allow to optimize the *in vitro* intracellular diffusion kinetic studies [24, 25]. Caco cells may be co-cultured with other cell types, such as fibroblasts, Goblet cells, and endothelial cells to generate more predictable models [24, 25]. This approach (requiring 21 d of co-culture) has been applied by using transwell insert systems [24–26], but its application to CELLBLOKS® system appeared to us not ease of manipulation for a potential industrial scale-up aimed to qualitatively study *in vitro* the potential ability of a neuroactive agent to reach the brain after OA.

As alternative to Caco cell lines, HIEC were suggested to replicate important properties of the human small intestine domain [27] but, unfortunately, the opportunity to obtain cell monolayers characterized by TEER values similar to those of human small intestine does not appear reproducible, because of the embryonic origin of this cell line [28].

The aspects above described induced us to choose the IEC-6 cells as simulated IB for the CELLBLOKS® system. The IEC are a non-transformed cell line derived from rat small intestinal cells, whose monolayers are characterized by TEER values comparable to the small intestine part of the ileum [24]. The effective permeability of compounds absorbed by paracellular or intercellular routes evidence values in the same order of magnitude in human and rat small intestine, even if slightly lower for rat species [25]. The IEC cells appeared therefore characterized by ease of manipulation to build a simulated IB in the CELLBLOKS® system, allowing to obtain a monolayer showing an acceptable correlation with human intestinal drug permeability, despite presenting interspecies variability [29, 30]. Specifically, we considered the correlation to be acceptable given the aim of our work, which proposes an *in vitro* model, relatively easy to handle, for a qualitative evaluation of the ability of potential neuroactive agents to reach the brain after having crossed the intestinal membrane and/or those between the bloodstream and the CNS.

In the CELLBLOKS® system, the specific microenvironments were simulated by seeding the cells on specific sides of the filter membranes of the barrier blocks. In particular, we considered that the basolateral side of both polarized endothelial and epithelial cells is involved in their adhesion to the filter membranes [31–33]. As a consequence, the channel simulating the bloodstream was constituted not only by its position below the three barrier blocks (figures 2 and 3), but also because it faced the apical side of hCMEC/D3 endothelial monolayer simulating the BBB and the basolateral side of HRPE and IEC-6 monolayers, simulating the BCSFB and IB, respectively. Likewise, the barrier blocks that replicate the brain parenchyma, CSF, and intestinal lumen were established not only by their position above the 'bloodstream' channel, but also because they faced the basolateral side of hCMEC/D3 endothelial monolayer and the apical side of HRPE and IEC-6 monolayers, respectively.

Despite the bloodstream faced *in vivo* the endothelial cells of the intestinal and BCSFB vessels, we have not replicated their presence in the CELLBLOKS® system; in other words, we did not seed them on the side of the barrier block filters which are opposite to those of HRPE and IEC-6 cells. We made this decision considering that the endothelial cells in the capillaries of choroid plexus lack tight junctions, allowing for the rapid passage through fenestrations of molecules of up to 12 nm [34, 35] and, similarly, the endothelial cells constituting the Gut Vascular Barrier display fenestrations that promote the rapid absorption of nutrients selected by the epithelial cells, preventing the passage into the bloodstream of bacteria and their derived products [36, 37].

As a consequence, the presence of the endothelial cells in the CELLBLOKS® system did not appear crucial in regulating the permeation of substances across the IB and BSCFB simulated by IEC-6 and HRPE cells, respectively. On the other hand, the absence of endothelial cells contributed to the relative ease of managing and reproducibility the CELLBLOKS® system, allowing to perform the permeation studies within a maximum of 12 d culture period after cell seeding.

To verify the suitability of cell monolayers as functional barrier in CELLBLOKS® system, the integrity of each of them was firstly assessed by measurements of their TEER values, considered indicative of their degree of tight and functional barrier. TEER is indeed a well-recognized measure of the ionic permeability of cell layers, which reveals the electrical capacitance of the barrier [23]. TEER can be related to several features of the cellular barriers, such as the amount and complexity degree of functional tight junctions and the expression of microvilli or other membrane invaginations. Consequently, TEER measurement is currently accepted as a non-invasive quantitative method able to reflect similarity to *in vivo* situations [23], providing the most selective approach to assess barrier integrity [38]. As shown in figure 4, the semipermeable membrane (polyethylene terephthalate material with 1 μm pore size) chosen as support for cell monolayers and constituting barrier blocks in the CELLBLOKS® platform appeared suitable for IEC-6, HRPE and hCMEC/D3 cell monolayers to develop TEER values comparable to those obtained in other commercial cell culture inserts for hCMEC/D3 cells ($\sim$60 Ω cm^2 in transwell corning inserts [39]) or HRPE cells ($\sim$80 Ω cm^2 in Millicell inserts [40]) or IEC-6 cells ($\sim$50 Ω cm^2 in cellQART inserts [41]).

Immunofluorescence staining has been also performed to assess the integrity of tight junctions in IEC-6, HRPE, and hCMEC/D3 cell monolayers cultured in CELLBLOKS®, including the zonula occludens (ZO) family of scaffolding proteins, namely ZO-1, and the family of tetraspan transmembrane proteins, such as occludin [14]. Immunofluorescence approach appears useful, indeed, as a complementary validation to the TEER measurements obtained from the same cell monolayers, enabling the correlation between protein expression and the functional tightness of the cellular barrier [15].

The immunofluorescence staining of ZO-1 protein and occludin evidenced their presence as distinct strands along the membrane of all three types of cell layers (figures S1(A) and (B)), aligning with their TEER values. Specifically, ZO-1 protein is recognized as a scaffolding protein, anchoring the tight junction to the actin component of the cytoskeleton and it appears necessary for the barrier polarisation [42]. Occludin, besides being another crucial protein for anchoring adjacent cells [15], is also involved in the preservation of cell surface polarity, allowing to restrict the diffusion of lipids in the outer leaflet of the plasma membrane [42]. The results reported in figures S1(A) and (B) suggest, therefore, that endothelial, intestinal, and choroid-like epithelial cells differentiated in the CELLBLOKS® system into functional cell monolayer and interacted with neighbouring cells in terms of cell-cell interactions. These monolayers were therefore considered appropriate in mimicking specific physiologic barriers *in vivo*.

In the CELLBLOKS® platform built as reported in figures 2 and 3, IVA or OA were simulated by introducing the compounds in the bloodstream-like channel or in the barrier blocks containing the intestinal (IEC-6 cells) monolayers, respectively. Then, sample withdrawal at fixed time points from the bloodstream-like channel allowed to study the permeability of the compounds across the IB, whereas sample withdrawal from the barrier blocks delimited by IB, BBB (hCMEC/D3 cells) or BCSFB (HRPE cells) monolayers allowed to evaluate the permeation ability of the compounds in the intestinal lumen (in the case of IVA simulation), brain parenchyma or the CSF, respectively, from the bloodstream.

As model compounds, celiprolol and eugenol were chosen taking into account their known different ability to permeate in the CNS from bloodstream *in vivo*: very poor for celiprolol [7] and very pronounced for eugenol [3].

These compounds were firstly studied in the CELLBLOKS® platform by simulating their IVA, considering that administration of drugs directly into the venous system, thereby circumventing the process of absorption, is utilized when an immediate drug effect or a very exact drug level in blood is required [43]. In this case the compounds were introduced in the blood mimetic channel at the final concentration of 7.5 μM, a value chosen because near to the highest plasmatic celiprolol concentration detected in the bloodstream of humans following its administration with doses higher than the normal therapeutic ones [16]. The concentration of eugenol introduced in the blood mimetic channel was the same for a direct comparison between the two compounds, despite this value is one order of magnitude lower to those found for eugenol in the bloodstream of rats after its intravenous infusion of 20 mg kg^{-1}, which allowed the permeation of this compound in the brain [3]. The concentration of 7.5 μM in the blood mimetic channel appeared, therefore, optimal to verify the ability of the barriers between blood and CNS to limit or allow, respectively, the permeation of celiprolol or eugenol toward the CNS compartments. Indeed, the celiprolol concentration in the blood channel was higher than those considered therapeutic in the

bloodstream of humans [16], whereas the concentration of eugenol was lower than that found in the rat after IVA which allowed its permeation into the CNS [3]. At these conditions, the cell monolayers mimicking the BBB and BCSFB appeared as efficacious barriers for the celiprolol permeation from the bloodstream-like channel to the CNS receiver compartments (figure 5(A)), whereas the presence of the same cell monolayers did not induce a decrease of the eugenol permeation (figure 6(A)). This aspect was further confirmed by considering the receiver recovery ratio (R/D ratio) values of the compounds permeating across the semipermeable membrane (filter) supporting the cell monolayers. In particular, as reported in figure 7, the R/D ratio values were calculated in the absence (cell-free filters) and in the presence of cell monolayers (filters with BBB or BCSFB). The R/D ratio values of celiprolol and eugenol permeating across the cell-free filters were almost the same, as indicated in table 1; in the presence of cell monolayers those of celiprolol were reduced to up about the 70% whereas those of eugenol were not significantly changed. Considering that the R/D ratio values are related to the distribution of the compounds mediated by the physiologic barriers between the central and blood compartments, the results related to IVA simulation of celiprolol and eugenol with the CELLBLOKS® platform indicate that the BBB and BCSFB represent strong barriers for the permeation of celiprolol from the blood compartment to the central compartments. On the other hand, the results obtained for eugenol indicate that BBB and BCSFB do not represent barriers able to significantly counteract its permeation from the blood compartment to the central-like receiver compartments, as reported in figure 7. These results appear in good agreement with literature data, indicating (*i*) celiprolol as a substrate of P-gp efflux systems, whose expression in the BBB and BCSFB strongly limits its permeation in the brain from the bloodstream [7] and (*ii*) eugenol as a compound able to easily permeate in the CNS following its IVA [3]. The behaviour of the simulated BBB and BCSFB in the CELLBLOKS® system towards celiprolol and eugenol does not appear influenced by the presence of the simulated IB, which appears able to counteract the permeation of these two compounds to its receiving compartment.

The simulated OA of celiprolol and eugenol in the CELLBLOKS® system allowed to further evidence the great difference of their ability to permeate in central compartments from the bloodstream. In this case the compounds were inserted in the IB block with a final concentration of 25 μM. This value was chosen being the highest possible eugenol concentration allowing to maintain the IEC-6 monolayer integrity, as indicated by TEER measurements by us performed. As a term comparison for permeation studies, the celiprolol concentration was therefore the same for OA simulation. TEER measurements of IEC-6 monolayers before and after 2 h of incubation with 25 μM celiprolol indicated that the monolayer integrity was not altered during the permeation experiments. The IEC-6 monolayer mimicking the IB evidenced their ability to counteract the permeation of both compounds (figures 5(B) and 6(B)), a result in good agreement with literature data indicating celiprolol as a substrate of efflux P-gp also for *in vivo* gastrointestinal absorption [44] and eugenol characterized by a poor oral bioavailability (about 4%) [3].

Interestingly, the celiprolol concentrations detected in the bloodstream-mimicking channel after the permeation across the IEC-6 monolayer ranged between about 0.6 and 0.9 μM (230 and 340 ng ml^{-1}). These values are very similar to the C_{max} values obtained in humans after the administration of therapeutic doses (100–200 mg, corresponding to about 1.5–3 mg kg^{-1}) [45, 46] or in rats after the administration of 10 mg kg^{-1} dose [47]). This condition appeared therefore suitable to evaluate *in vitro* the aptitude of celiprolol to target the simulated central compartments, evidencing its inability to permeate from the bloodstream-mimicking channel of the CELLBLOKS® platform to the central-mimicked receiver compartments (figure 5(C)) by R/D ratio values equal to zero. This result is in good agreement with literature data which describe celiprolol as a drug widely distributed in all tissues, with the exception of the brain, after absorption of therapeutic doses [16].

The eugenol concentrations detected in the bloodstream-mimicking channel after the permeation across the IEC-6 monolayer ranged between about 0.8 and 1 μM (140 and 160 ng ml^{-1}), showing similar values of celiprolol at the same conditions. These concentrations were poor in comparison to those of eugenol detected in the bloodstream of rats after an OA of a 500 mg kg^{-1} dose, where the C_{max} value was about 20 μM (3.4 μg ml^{-1}) [3]. This condition appeared optimal in order to evaluate the ability of the CELLBLOKS® platform to indicate the eugenol aptitude to permeate in the CNS from the bloodstream after the simulated OA. Accordingly, despite its relatively low concentration in the bloodstream-mimicking channel of the CELLBLOKS® platform, eugenol appeared able to permeate to the CNS-like receiver compartments (figure 6(C)), evidencing R/D ratio values significantly higher than zero (ranging between about 0.1 and 0.2). These data, obtained after the simulation of OA, confirm the marked aptitude of eugenol to permeate from the bloodstream to the CNS, as previously found by IVA simulation. This result is in good agreement with literature data that indicate eugenol able to permeate in the CSF of rats after the administration of an oral dose designed to inhibit its absorption in the bloodstream, where the plasmatic C_{max} value of eugenol was limited to 1.4 μM (0.23 μg ml^{-1}) [3], a value of the same order of magnitude of the concentrations

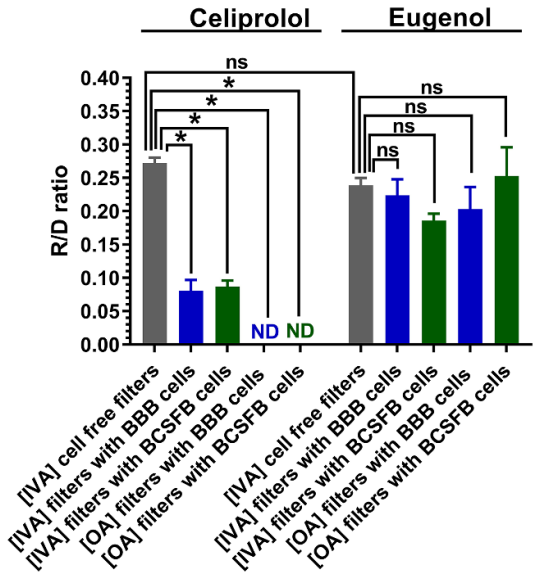

Figure 9. Receiver recovery ratio (R/D ratio) values obtained for celiprolol or eugenol after two hours of incubation in the CELLBLOKS® system, where they permeated from the blood-mimicking channel to central-mimicking compartments delimitated by cell monolayers (BBB or BCSFB cells). The R/D ratio values were obtained after IVA simulation in the absence (cell-free filters) or in the presence of cell monolayers (filters with BBB or BCSB cells) and after OA simulation in the presence of cell monolayers. Data are expressed as the mean ± SEM of four independent experiments. * $P < 0.0001$; ns = no significant difference; ND = no detected.

found in bloodstream-mimicking channel after OA simulation.

The strong different ability between celiprolol and eugenol to permeate the BBB or BCSFB mimicked by the CELLBLOKS® system can be summarized in figure 9, where the recovery ratio (R/D ratio) of these compounds in the central receiver compartments permeating from the blood-mimicking channel are reported after two hours of their incubation in the absence or in the presence of cell monolayers. In particular, after IVA simulation in the absence of cell monolayers the R/D values of celiprolol and eugenol did not appear significantly different from each other, showing values about 0.25. These R/D values were not significantly changed, in the case of eugenol, by the presence of the mimicked BBB or BCSFB, when both IVA and OA were simulated in the CELLBLOKS® system, evidencing that these barriers did not counteract the eugenol permeation from the mimicked-bloodstream channel to mimicked-central levels. On the contrary, the presence of cell monolayers mimicking the BBB or BCSFB was detrimental for the celiprolol permeation in the central receiver compartments, as evidenced by the R/D values strongly lowered to about 0.04 after IVA simulation or reduced to zero after OA simulation.

The ability of eugenol to permeate across the simulated BBB and BCSFB monolayers was further confirmed by its aptitude to induce DA release from neuronal-like differentiated PC12 cells located on NANOSTACKS™, as reported in figures 2 and 3. We have evidenced that the presence of IB in the CELLBLOKS® system does not influence the ability of eugenol to permeate across the simulated BBB and BCSFB; as a consequence the IVA simulation for this study was performed using the CELLBLOKS® system with the configuration obtained in the absence of IEC-6 cells (as represented in figure 3(A2)). The PC12 cell line was chosen to simulate the dopaminergic neurons, despite the rat origin, because recognized as an essential tool for the nervous system investigation. In particular, PC12 cells can be easily differentiated into neuron-like cells upon NGF exposure [48] and they are characterized by neurosecretory capabilities (norepinephrine, catecholamines and DA) [49]. This cell line was therefore preferred to others of human origin, such as SH-SY5Y and IMR-32, derived from neuroblastoma and evidencing several limitations due to death and loss during splitting and manipulation. In general, PC12 cells are preferred for DA release studies (being derived from rat adrenal medulla) with respect to SH-SY5Y cells, requiring more efforts to develop a strong dopaminergic phenotype [50]. These reasons led us to consider PC12 cells as a model relatively easy to handle and suitable to evaluate the ability of eugenol to induce central effects after its simulated permeation through blood-CNS barriers. It is noteworthy that the eugenol-induced DA release from PC12 cells inside the BBB- or BCSFB-delimited compartments was comparable at the same incubation time (60 or 120 min) both in IVA and OA simulated conditions, although the eugenol concentrations reached at the same incubation time (60 or 120 min) were significantly different between simulated IVA and OA ($P < 0.01$). This *in vitro* evidence could provide a good prospective index of penetration in the CNS of eugenol.

As reported in figure 8, it is noteworthy that following simulated IVA and OA, the eugenol concentration in the BBB- and BCSFB-delimited compartments doubled or remained statistically unchanged from 60 to 120 min, respectively, while DA release from PC12 placed in the same compartments increased up to 6.5-fold after IVA and up to 6-fold after OA. The observed insignificant contribution of baseline to the eugenol-stimulated DA release from PC12 cells allows us to rule out time-dependent changes in DA release. Moreover, the specificity of eugenol-induced release is strengthened by considering nomifensine and pargyline, both inserted in DA release buffer as DA reuptake and monoamine oxidase inhibitors, respectively, unable to stimulate DA release. Nomifensine and pargyline have been indeed reported as very poorly efficacious in increasing basal concentrations of DA. In particular, a combination of pargyline and nomifensine evidenced a slight accumulation of basal DA release [51, 52]. Our

results appear in good agreement with this behaviour, allowing us to consider the two compounds as negative control on DA release in comparison to the neurotropic agent eugenol. In addition, eugenol-stimulated DA release is consistent with the time- and concentration-dependent hormetic behaviour of eugenol in inducing DA release from PC12 cells, which showed a biphasic U-shaped trend, as previously described [3]. In the present work, time-dependent hormesis of eugenol-induced DA release from PC12 cells can be clearly observed in simulated OA, while concentration-dependent hormesis is evident as the lowest eugenol concentrations reached in OA induced similar DA release as the highest eugenol concentrations reached in IVA. The U–shape of dose-response relationships in neurobiological systems have been already documented [53]. Due to the hormetic dose-response relationship for eugenol efficacy, therefore, we can argue that a lower dose of eugenol in IVA may be sufficient to achieve the same effect as OA-derived eugenol. The hormetic effects are believed to support, strengthen and optimize normal neurological functions, and protect the brain from a variety of metabolic, neurodegenerative and traumatic injuries [53]. Based on its behaviour on dopaminergic neuron-like PC12 cells, eugenol could therefore be included among the hormesis-based pharmacological treatments in the dynamics of DA release involved in brain functions *in vivo*, such as reward, mood, and attention.

5. Conclusion

In conclusion, the results described here validate the CELLBLOKS® and NANOSTACKS™ platforms as *in vitro* robust tools for studying the transport of new neuroactive drugs across physiological barriers and their functional effects on CNS-like tissues after their IVA or OA. In particular, the proposed platform appears relatively easy to handle, being based on cellular lines requiring around two weeks culture period to be ready for the simulation *in vitro* of IB, BBB, BCFSB, and neuronal tissues, allowing measurements that can be performed via HPLC for permeation studies. The BBB and BCFSB are simulated by cells of human origin which contribute to reduce the interspecies variability related to permeation studies of potential new neuroactive agents in the CNS. The IB is simulated by cells of rodent origin, characterized by ease of manipulation. These cells should anyway allow an acceptable correlation with human intestinal drug permeability in view of the use of this platform, which is designed for a qualitative evaluation of the ability of potential neuroactive agents to reach the brain after having crossed the intestinal membrane and/or those between the bloodstream and the CNS. The platform can also allow to verify potential functional effects of neuroactive agents on simulated CNS tissues after mimicking their BBB or BCSFB crossing. In this case, PC12 cells were grown and differentiated to dopaminergic neurons on NANOSTACKS™ where they released DA after interaction with eugenol, which targeted them after intravenous or oral mimicked administration. The PC12 cell line has rodent origins, but offers ease of differentiation into neuron-like cells, in comparison to human cell lines derived from neuroblastoma; moreover, the opportunity of verifying from a qualitative point of view the existence of central effects, should be independent on the origin species of the neuronal cells used.

The current results support therefore the reliability of the CELLBLOKS® system to study *in vitro* the ability of new potential neuroactive agents to permeate in the brain before performing their *in vivo* IVA or OA, laying the basis for the development of an effective *in vitro-in vivo* correlation (IVIVC) that may allow the reduction of animal use in research. This platform may be proposed for a first *in vitro* screening in order to select new neuroactive agents potentially able to reach the brain after crossing the IB and BBB or BCSFB, following OA and/or IVA.

As further perspective, the reliability of this CELLBLOKS® system could be additionally improved following two strategies: *(i)* the use of 3D cellular models on the filters of the barrier blocks and on NANOSTACKS™; *(ii)* by incorporating gastrointestinal and plasma enzyme pools, alongside hepatic cell models to simulate first-pass metabolism in oral drug administration. The improved platforms could allow to obtain *in vitro* more accurate and qualitative data on the potential neuronal activity of the drugs selected by the first screening performed with the platform proposed in this article.

Acknowledgment

Supports from the University of Ferrara, Italy (grant no. 2022-FAR.L-DA_018), are gratefully acknowledged.

Data availability statement

All data that support the findings of this study are included within the article (and any supplementary files).

Supplementary figures available at https://doi.org/10.1088/1758-5090/ae514c/data1.

Conflict of interest

The authors declare that they have no known competing financial interests or personal relationships that could have appeared to influence the work reported in this paper.

Author contributions

Barbara Pavan 0000-0001-8942-9310
Conceptualization (equal), Data curation (equal), Formal analysis (equal), Investigation (equal), Methodology (equal), Project administration (equal), Supervision (equal), Validation (equal), Visualization (equal), Writing – original draft (equal), Writing – review & editing (equal)

Giada Botti 0000-0002-2942-1437
Data curation (equal), Formal analysis (equal), Investigation (equal), Validation (equal), Visualization (equal), Writing – original draft (equal), Writing – review & editing (equal)

Alessandro Dalpiaz 0000-0002-6648-2562
Conceptualization (equal), Data curation (equal), Formal analysis (equal), Funding acquisition (equal), Investigation (equal), Methodology (equal), Project administration (equal), Resources (equal), Supervision (equal), Validation (equal), Visualization (equal), Writing – original draft (equal), Writing – review & editing (equal)

Raffaello Sbordoni 0009-0003-5791-3652
Conceptualization (equal), Investigation (equal), Methodology (equal)

Abdullah Talari 0000-0002-0275-9876
Methodology (equal), Writing – review & editing (supporting)

Valon Llabjani 0000-0001-6541-355X
Conceptualization (equal), Methodology (equal), Resources (equal), Supervision (equal), Validation (equal), Writing – review & editing (equal)

References

[1] Pavan B and Dalpiaz A 2011 Prodrugs and endogenous transporters: are they suitable tools for drug targeting into the central nervous system? *Curr. Pharm. Des.* **17** 3560–76
[2] Sanchez-Covarrubias L, Slosky L M, Thompson B J, Davis T P and Ronaldson P T 2014 Transporters at CNS barrier sites: obstacles or opportunities for drug delivery? *Curr. Pharm. Des.* **20** 1422–49
[3] Pavan B, Bianchi A, Botti G, Ferraro L, Valerii M C, Spisni E and Dalpiaz A 2023 Pharmacokinetic and permeation studies in rat brain of natural compounds led to investigate eugenol as direct activator of dopamine release in PC12 cells *Int. J. Mol. Sci.* **24** 1800
[4] Llabjani V, Siddique M R, Macos A, Abouzid A, Hoti V, Martin F L, Patel I I and Raza A 2022 Introducing CELLBLOKS®: a novel organ-on-a-chip platform allowing a plug-and-play approach towards building organotypic models *Vitro Model.* **1** 423–35
[5] Talari A, Sbordoni R, Jalil T, Patel I, Martin F, Raza A and Llabjani V 2025 Multicellular hepatic *in vitro* models using NANOSTACKS™: human-relevant models for drug response prediction *In vitro models* **18** 1–4
[6] Pavan B, Bianchi A and Botti G 2022 *In vitro* cell models merging circadian rhythms and brain waves for personalized neuromedicine *iScience* **25** 105477
[7] Milne R J and Buckley M M 1991 Celiprolol. An updated review of its pharmacodynamic and pharmacokinetic properties, and therapeutic efficacy in cardiovascular disease *Drugs* **41** 941–69
[8] Arias-Carrión O, Stamelou M, Murillo-Rodríguez E, Menéndez-González M and Pöppel E 2010 Dopaminergic reward system: a short integrative review *Int. Arch. Med.* **3** 24
[9] Carloni S and Rescigno M 2022 Unveiling the gut-brain axis: structural and functional analogies between the gut and the choroid plexus vascular and immune barriers *Sem. Immunopathol.* **44** 869–82
[10] Scalise A A, Kakogiannos N, Zanardi F, Iannelli F and Giannotta M 2021 The blood-brain and gut-vascular barriers: from the perspective of claudins *Tissue Barriers* **9** 1926190
[11] Gorgels T G M F and Bergen A A B Choroid plexus and retinal pigment epithelium: two of a kind? (available at: www.brainbank.nl/media/uploads/file/Gorgels2.pdf)
[12] Rizzolo L J 2007 Development and role of tight junctions in the retinal pigment epithelium *Int. Rev. Cytol.* **258** 195–234
[13] Schimetz J, Shah P, Keese C, Dehnert C, Detweiler M, Michael S, Toniatti-Yanulavich C, Xu X and Padilha E C 2024 Automated measurement of transepithelial electrical resistance (TEER) in 96-well transwells using ECIS TEER96: single and multiple time point assessments *SLAS Technol.* **29** 100116
[14] Zihni C, Mills C, Matter K and Balda M S 2016 Tight junctions: from simple barriers to multifunctional molecular gates *Nat. Rev. Mol. Cell Biol.* **17** 564–80
[15] Ross A M, Walsh D R, Cahalane R M, Marcar L and Mulvihill J J E 2021 The effect of serum starvation on tight junctional proteins and barrier formation in Caco-2 cells *Biochem. Biophys. Reports* **27** 101096
[16] Nawarskas J J, Cheng-Lai A and Frishman W H 2017 Celiprolol: a unique selective adrenoceptor modulator *Cardiol. Rev.* **25** 247–53
[17] Li L *et al* 2022 Permeability-engineered compartmentalization enables in vitro reconstitution of sustained synthetic biology systems *Adv. Sci.* **9** e2203652
[18] Xavier M, Rodrigues P M, Neto M D, Guedes M I, Calero V, Pastrana L and Gonçalves C 2023 From mouth to gut: microfluidic *in vitro* simulation of human gastro-intestinal digestion and intestinal permeability *Analyst* **148** 3193–203
[19] Weksler B, Romero I A and Couraud P O 2013 The hCMEC/D3 cell line as a model of the human blood brain barrier *Fluids Barriers CNS* **10** 16
[20] Hu J and Bok D 2014 The use of cultured human fetal retinal pigment epithelium in studies of the classical retinoid visual cycle and retinoid-based disease processes *Exp. Eye Res.* **126** 46–50
[21] Philp N J, Yoon H and Lombardi L 2001 Mouse MCT3 gene is expressed preferentially in retinal pigment and choroid plexus epithelia *Am. J. Physiol. Cell Physiol.* **280** C1319–26
[22] Redzic Z B 2013 Studies on the human choroid plexus in vitro *Fluids Barriers CNS* **10** 10
[23] Dabbagh F, Schroten H and Schwerk C 2022 In vitro models of the blood-cerebrospinal fluid barrier and their applications in the development and research of (neuro)pharmaceuticals *Pharmaceutics* **14** 1729
[24] Fedi A, Vitale C, Ponschin G, Ayehunie S, Fato M and Scaglione S 2021 In vitro models replicating the human intestinal epithelium for absorption and metabolism studies: a systematic review *J. Control. Release* **335** 247–68
[25] Macedo M H, Barros A S, Martínez E, Barrias C C and Sarmento B 2022 All layers matter: innovative three-dimensional epithelium-stroma-endothelium intestinal model for reliable permeability outcomes *J. Control. Release* **341** 414–30
[26] Zeiringer S, Wiltschko L, Glader C, Reiser M, Absenger-Novak M, Fröhlich E and Roblegg E 2023 Development and

characterization of an in vitro intestinal model including extracellular matrix and macrovascular endothelium *Mol. Pharm.* **20** 5173–84
[27] Takenaka T, Harada N, Kuze J, Chiba M, Iwao T and Matsunaga T 2014 Human small intestinal epithelial cells differentiated from adult intestinal stem cells as a novel system for predicting oral drug absorption in humans *Drug Metab. Dispos.* **42** 1947–54
[28] Lopez-Escalera S and Wellejus A 2022 Evaluation of Caco-2 and human intestinal epithelial cells as *in vitro* models of colonic and small intestinal integrity *Biochem. Biophys. Reports* **31** 101314
[29] Wolf T, Baier S R and Zempleni J 2015 The intestinal transport of bovine milk exosomes is mediated by endocytosis in human colon carcinoma Caco-2 cells and rat small intestinal IEC-6 cells *J. Nutr.* **145** 2201–6
[30] Lee Y, Kim Y, Park S, Heo G, Chung H Y and Im E 2023 Cannabinoid receptor type 1 in the aging gut regulates the mucosal permeability via miR-191-5p *Front. Endocrinol* **14** 1241097
[31] Stone N L, England T J and O'Sullivan S E 2019 A novel transwell blood brain barrier model using primary human cells *Front. Cell Neurosci.* **13** 230
[32] Franco Y L, Da Silva L and Cristofoletti R 2021 Navigating through cell-based in vitro models available for prediction of intestinal permeability and metabolism: are we ready for 3D? *AAPS J.* **24** 2
[33] Mancinelli E, Zushi N, Takuma M, Cheng Chau C C, Parpas G, Fujie T and Pensabene V 2024 Porous polymeric nanofilms for recreating the basement membrane in an endothelial barrier-on-chip *ACS Appl. Mater. Interfaces* **16** 13006–17
[34] Johnsen L Ø, Friis K A, Møller-Madsen M K and Damkier H H 2025 Mechanisms of cerebrospinal fluid secretion by the choroid plexus epithelium: application to various intracranial pathologies *Clin. Anat.* **38** 63–74
[35] Katada S, Rodrigues K S and Nakashima K 2025 The influence of the choroid plexus on brain function: beyond its role in cerebrospinal fluid production *Inflamm Regen.* **45** 20
[36] Brescia P and Rescigno M 2021 The gut vascular barrier: a new player in the gut-liver-brain axis *Trends Mol. Med.* **27** 844–55
[37] Bernier-Latmani J, González-Loyola A and Petrova T V 2024 Mechanisms and functions of intestinal vascular specialization *J. Exp. Med.* **221** e20222008
[38] Srinivasan B, Kolli A R, Esch M B, Abaci H E, Shuler M L and Hickman J J 2015 TEER measurement techniques for in vitro barrier model systems *J. Lab Autom.* **20** 107–26
[39] Weksler B B *et al* 2005 Blood-brain barrier-specific properties of a human adult brain endothelial cell line *FASEB J.* **19** 1872–4
[40] Dalpiaz A, Paganetto G, Pavan B, Fogagnolo M, Medici A, Beggiato S and Perrone D 2012 Zidovudine and ursodeoxycholic acid conjugation: design of a new prodrug potentially able to bypass the active efflux transport systems of the central nervous system *Mol. Pharm.* **9** 957–68
[41] Faiella M, Botti G, Dalpiaz A, Gnudi L, Goyenvalle A, Pavan B, Perrone D, Bovolenta M and Marchesi E 2024 In vitro studies to evaluate the intestinal permeation of an ursodeoxycholic acid-conjugated oligonucleotide for Duchenne Muscular Dystrophy treatment *Pharmaceutics* **16** 1023
[42] Zheng X, Ren B and Gao Y 2023 Tight junction proteins related to blood-brain barrier and their regulatory signaling pathways in ischemic stroke *Biomed. Pharmacother.* **165** 115272
[43] Sultatos L 2007 Routes of drug administration *xPharm: The Comprehensive Pharmacology Reference* ed S J Enna and D B Bylund (Elsevier) pp 1–3
[44] Kato Y, Miyazaki T, Kano T, Sugiura T, Kubo Y and Tsuji A 2009 Involvement of influx and efflux transport systems in gastrointestinal absorption of celiprolol *J. Pharm. Sci.* **98** 2529–39
[45] Hartmann C, Frölich M, Krauss D, Spahn-Langguth H, Knauf H and Mutschler E 1990 Comparative enantioselective pharmacokinetic studies of celiprolol in healthy volunteers and patients with impaired renal function *Eur. J. Clin. Pharmacol.* **39** 573–6
[46] Lilja J J, Backman J T, Laitila J, Luurila H and Neuvonen P J 2003 Itraconazole increases but grapefruit juice greatly decreases plasma concentrations of celiprolol *Clin. Pharmacol. Ther.* **73** 192–8
[47] Miyazaki N, Misaka S, Ogata H, Fukushima T and Kimura J 2013 Effects of itraconazole, dexamethasone and naringin on the pharmacokinetics of nadolol in rats *Drug Metab. Pharmacokinet* **28** 356–61
[48] Zhong Y, Liu M M, Li J C, Lu T C, Cao X, Yang Y J, Lei Y and Liu A L 2024 In vitro drug screening models derived from different PC12 cell lines for exploring Parkinson's disease based on electrochemical signals of catecholamine neurotransmitters *Mikrochim. Acta* **191** 170
[49] Wang W L, Dai R, Yan H W, Han C N, Liu L S and Duan X H 2015 Current situation of PC12 cell use in neuronal injury study *Int. J. Biotechnol. Wellness Ind.* **4** 61–66
[50] Oprea D, Sanz C G, Barsan M M and Enache T A 2022 PC-12 cell line as a neuronal cell model for biosensing applications *Biosensors* **12** 500
[51] Garris P A and Ben-Jonathan N 1991 Effects of reuptake inhibitors on dopamine release from the stalk-median eminence and posterior pituitary in vitro *Brain Res.* **556** 123–9
[52] Blaha C D, Coury A and Phillips A G 1996 Does monoamine oxidase inhibition by pargyline increase extracellular dopamine concentrations in the striatum? *Neuroscience* **75** 543–50
[53] Calabrese E J, Calabrese V and Giordano J 2017 The role of hormesis in the functional performance and protection of neural systems *Brain Circ.* **3** 1–13